(54) Title: FLUORESCENCE-MEDIATED MOLECULAR TOMOGRAPHY

(57) Abstract: This invention relates to a fluorescence-mediated molecular tomographic imaging system, designed to detect near-infrared fluorescence activation in deep tissues. The system can use targeted fluorescent molecular probes or highly sensitive activatable fluorescence molecular probes. Such probes add molecular specifity and yield high fluorescence contrast, to allow early detection and molecular target assessment of diseased tissue, such as cancers, in vivo. The new tomographic imaging system enable three-dimensional localization in deep tissues and quantitation of molecular probes.

WO 02/41760 A2

(BF, BJ, CF, CG, CI, CM, GA, GN, GQ, GW, ML, MR, NE, SN, TD, TG).

Published:

— *without international search report and to be republished upon receipt of that report*

For two-letter codes and other abbreviations, refer to the "Guidance Notes on Codes and Abbreviations" appearing at the beginning of each regular issue of the PCT Gazette.

FLUORESCENCE-MEDIATED MOLECULAR TOMOGRAPHY

TECHNICAL FIELD

This invention relates to extracting quantitative, three-dimensional molecular information from living mammals and patients using fluorochromes and new optical tomographic imaging methods.

BACKGROUND

Molecular imaging can be broadly defined as the characterization and measurement of biological processes at the cellular and molecular level in mammals and human patients. In contradistinction to "classical" diagnostic imaging, for example, magnetic resonance (MR), computed tomography (CT), and ultrasound (US) imaging, molecular imaging analyses molecular abnormalities that are the basis of disease, rather than imaging the end-effects of these molecular alterations. Specific imaging of molecular targets allows earlier detection and characterization of disease, as well as earlier and direct molecular assessment of treatment efficacy. Molecular imaging can theoretically be performed with different imaging technologies, up to now preferably with nuclear imaging technologies, e.g., PET and SPECT imaging) which have high sensitivity of probe detection. The IV administered imaging probes typically recognize a given target. Alternatively, some probes detectable by MR imaging have been developed (Moats et al., Angewandte Chemie Int. Ed., 36:726-731, 1997; Weissleder et al., Nat. Med., 6:351-5, 2000), although their detection threshold is generally in the micromolar instead of the pico/femptomolar range of isotope probes.

An alternative method is to use fluorescent probes for target recognition. For example, enzyme activatable fluorochrome probes are described in Weissleder et al., U.S. Patent No. 6,083,486, and fluorescent molecular beacons that become fluorescent after DNA hybridization are described in Tyagi et al., Nat. Biotechnol., 16:49-53, 1998. Fluorescence activatable probes have been used in tissue culture and histologic sections and detected using fluorescence microscopy. When administered in vivo, fluorescence activatable probes have been detected by surface-weighted reflectance imaging (Weissleder et al., Nat. Biotechnol., 17:375-8, 1999); Mahmood et al., Radiology, 213:866-70, 1999. However, imaging in deep tissues (> 5 mm from the surface), in absorbing and scattering media such as mammalian

tissues, and quantitating fluorescence (and in particular fluorescence activation) has not been described.

To image light interactions in deeper tissues, light in the near infrared (near-IR or NIR) instead of the visible spectrum is preferred. Imaging with near infrared (near-IR or NIR) light has been in the frontier of research for resolving and quantifying tissue function. Light offers unique contrast mechanisms that can be based on absorption, e.g., probing of hemoglobin concentration or blood saturation, and/or fluorescence, e.g., probing for weak auto-fluorescence, or exogenously administered fluorescent probes (Neri et al., Nat. Biotech., 15:1271-1275, 1997; Ballou et al., Cancer Immunol. Immunother., 41:257-63,1995; and Weissleder, 1999). In either application, NIR photons undergo significant elastic scattering when traveling through tissue. This results in light "diffusion" in tissue that hinders resolution and impairs the ability to produce diagnostically interpretable images using simple "projection" approaches (transillumination), as in x-ray imaging.

During the last decade, mathematical modeling of light propagation in tissue, combined with technological advancements in photon sources and detection techniques has made possible the application of tomographic principles (Kak and Slaney, "Principles of Computerized Tomographic Imaging," IEEE Press, New York, 1988, pp. 208-218); Arridge, Inverse Problems, 15:R41-R93, 1999) for imaging with diffuse light. Diffuse Optical Tomography (DOT) uses multiple projections and deconvolves the scattering effect of tissue. DOT imaging has been used for quantitative, three-dimensional imaging of intrinsic absorption and scattering (see, e.g., Ntziachristos et al., Proc. Natl. Acad. Sci., USA, 97:2767-72, 2000, and also Benaron et al., J. Cerebral Blood Flow Metabol., 20(3):469-77, 2000). These fundamental quantities can be used to derive tissue oxy- and deoxy-hemoglobin concentrations, blood oxygen saturation (Li et al., Appl. Opt., 35:3746-3758, 1996) or hematoma detection in diffuse media.

Although intrinsic-contrast for DOT imaging may be useful in certain situations, e.g., for functional brain activation studies or hematoma detection, these applications do not allow the extraction of highly specific molecular information from living tissues. Fluorochrome concentration has been measured by absorption measurements (Ntziachristos et al., 2000) or by fluorescence measurements in phantoms (Chang et al., IEEE Trans. Med. Imag., 16:68-77, 1997; Sevick-Muraca et al., Photochem. Photobiol., 66:55-64, 1997). However,

2

previously described DOT systems and/or image algorithms have not been useful to obtain three-dimensional quantitation of fluorescence in deep tissues in living mammals.

SUMMARY

The invention is based on the discovery that in vivo fluorochrome signals from a variety of molecular probes, such as specific targeted molecular probes, e.g., probes targeted for specific enzyme activities or DNA sequences, can be localized in three dimensions in deep tissues and can be quantitated with high sensitivity using a specially designed imaging system for this purpose and relying on self-calibrated image reconstruction and new algorithms to extract molecular maps.

In general, the invention features a fluorescence-mediated molecular tomography (FMT) imaging system that includes a light source (e.g., an NIR or visible light source) to provide incident light; a multipoint incident illumination array to direct light into an object, e.g., an animal or human patient, from two or more separate excitation points; multiple optic fibers to transmit light from the light source to each point in the multipoint incident illumination array; a multipoint detection array to collect light, e.g., fluorescent light, emitted from the object from two or more separate collection points; a two-dimensional emitted light array to transmit light emitted from the object to a detector; multiple optic fibers to transmit light from each collection point to a corresponding point on the two-dimensional emitted light array; and a detector to detect and convert light emitted from each point of the two-dimensional emitted light array into a digital signal corresponding to the light emitted from the object.

In this system, the emitted light can be continuous wave (CW) light, time-resolved (TR) light, intensity modulated (IM) light, or any combination of the above.

The system can further include a processor that processes the digital signal produced by the detector to provide an image on an output device. The output device can provide multiple images simultaneously. The processor can be programmed to process the digital signal by any one or combinations of: i) generating a corrected fluorescence measurement by subtracting a background signal and filter bleed-through signal from collected fluorescence measurements; ii) generating a corrected intrinsic signal measurement by subtracting a background ambient light signal from collected intrinsic signal measurements; iii) generating

3

a self-calibrated fluorescence measurement by dividing the corrected fluorescence measurement by the corrected intrinsic measurement; iv) generating a corrected background-medium diffuse signal by subtracting the collected background ambient light signal from a collected diffuse signal; and v) generating a self-calibrated intrinsic measurement by dividing
5   the corrected intrinsic signal measurement by the corrected background-medium diffuse signal.

In other embodiments, the processor can be programmed to process the digital signal by any one or combinations of: i) generating a self-calibrated measurement $M = M1 - M3 / M2 - M4$, or another function of M, wherein M1 is an emission wavelength fluorescence
10   signal, M2 is an intrinsic signal, M3 is a fluorescence background and/or bleed-through signal, M4 is an intrinsic wavelength background ambient light signal; ii) generating a self-calibrated intrinsic measurement $M' = \log (M2 - M4)/(M5 - M4)$, or some other function of M', wherein M5 is a background-medium diffuse signal; iii) minimizing a function $F(U) = (M - P \times U)^2$, or any other function of $(M - P \times U)$ (such as the absolute value, or cubed
15   value), to obtain a distribution and magnitude of U, wherein U is a spatially dependent vector of unknown fluorochrome concentration and/or fluorochrome lifetime within the volume imaged, and P is a forward predictor of M calculated by solving the transport equation, or an approximation of the transport equation such as the diffusion equation, for an appropriate geometry and background medium in the appropriate mode that M is constructed; iv)
20   minimizing a function $F'(O) = (M' - P' \times O)^2$ or functions of $(M'-P' \times O)$ to obtain a distribution and magnitude of O; wherein O is a vector of unknown absorption of a fluorophore in the object, and P' is a forward predictor of M' calculated by solving the transport equation or an approximation of it such as the diffusion equation for the appropriate geometry and background medium in the appropriate absorption/scattering mode; v)
25   calculating an activation ratio $AR = U/O$; and vi) generating an image corresponding to AR.

The measurement M3 can be experimentally obtained using calibration media or can be estimated or calculated based on the field M2. In particular, the measurement can be written as $M3 = q1(r) \times M2 + ct$, where q1 is the filter attenuation of the intrinsic field and is a spatially dependent factor that can account for radially dependent filter anisotropy. The
30   factor q1(r) can be determined experimentally by flat field measurements or calculated based of filter specifications. The constant ct represents an image of the background dark noise

4

measurement of the CCD camera. In addition, M3 can be written as $M3 = q1(r) \times M2' + ct$, where M2' is theoretically calculated using a solution of the transport equation or an approximation of it such as the diffusion equation for a homogeneous medium with the average optical properties of the medium of investigation or for a heterogeneous medium obtained by using known information.

The imaging system can include more than 100 optic fibers to transmit light into the patient and/or from each collection point of the detection array, and the detector array can include at least 100 collection points.

In this imaging system, the two-dimensional emitted light array can transmit to the detector a two-dimensional pattern of multiple points of light corresponding to light emitted from the patient in three-dimensions, wherein the pattern varies over time at a rate corresponding to switching of illumination from one to another of the two or more excitation points. In addition, the two or more excitation points are illuminated by the light source one at a time. In certain embodiments the NIR light directed into the object can be at a wavelength of from 550 to 950, e.g., 670 or 750 to 850, nanometers, and the detector can be a charge-coupled device (CCD) camera or can include photomultiplier tubes.

The system can also include molecular probes, such as NIR fluorescent (NIRF) molecular probes, themselves. The probes can be activatable molecular probes.

The invention also features a method for displaying i) a fluorochrome distribution and/or lifetime as resolved by vector U and/or ii) an optical molecular map corresponding to a ratio of a concentration of a molecular probe comprising a fluorophore administered to a patient to a concentration of an activated fluorophore corresponding to a specific target in the patient by: i) providing a first data set of fluorophore concentration based on intrinsic absorption; ii) providing a second data set of activated fluorophore concentration based on fluorescence; iii) dividing the first data set by the second data set on a point-by-point basis to provide a third data set; and iv) processing the third data set to provide an optical molecular map corresponding to a ratio of a concentration of a molecular probe comprising a fluorophore to a concentration of an activated fluorophore corresponding to a specific target in the patient.

In another aspect, the invention features a method of obtaining a three-dimensional, quantitative, molecular tomographic image of a target region within a patient, by

5

administering a near-infrared fluorescent (NIRF) molecular probe to the patient, wherein the molecular probe selectively accumulates within a target region in the patient; directing near-infrared light from multiple points into the patient; detecting fluorescent light emitted from the patient; and processing the detected light to provide a three-dimensional image that

5   corresponds to the three-dimensional target region within the patient and to the quantity of molecular probe accumulated in the target region.

In this method, the three-dimensional image can be visualized on a two-dimensional output device. The processing can include digitizing the fluorescent signal emitted from the patient, self-calibrating the digital signal by combining fluorescent and intrinsic signal

10   measurements from the patient and background medium, and reconstructing a three-dimensional, quantitative image. In certain embodiments, the processing includes i) generating a corrected fluorescence measurement by subtracting a background signal and filter bleed-through signal from collected fluorescence measurements; ii) generating a corrected intrinsic signal measurement by subtracting a background ambient light signal from

15   collected intrinsic signal measurements; iii) generating a self-calibrated fluorescence measurement by dividing the corrected fluorescence measurement by the corrected intrinsic measurement; iv) generating a corrected background-medium diffuse signal by subtracting the collected background ambient light signal from a collected diffuse signal; and v) generating a self-calibrated intrinsic measurement by dividing the corrected intrinsic signal

20   measurement by the corrected background-medium diffuse signal.

The processing can also include other steps described herein. In these methods, the molecular probes can be administered systemically or locally by injecting a molecular probe, e.g., an activatable probe. The molecular probe can be locally injected into the target region or into a non-target region, for example, by intraperitoenal administration with systemic

25   absorption and administration by an implanted slow-release compound or device such as a pump.

In certain embodiments of the new methods, the NIR light can be directed into the patient from separate points of light (e.g., 12, 24, 32, or more points) arranged in a fixed three-dimensional geometry, or with a multipoint incident illumination array comprising a

30   belt having independent points of light (e.g., at least 12 or more points). In addition, the spatial localizations of the multipoint incident illumination array and the multipoint detector

6

array can be determined by image co-registration. In other embodiments, photon pulses are directed into the patient and the arrival of photons emitted from the patient is time-resolved using a separate array of photon detectors or time-gated intensified CCD camera (iCCD). Similar detection can be achieved using when using light of modulated intensity employing an iCCD camera and a demodulation arrangement directed onto the image intensifier in a manner similar to dynode demodulation techniques often applied to photo-multiplier tube demodulation.

The emitted fluorescent light in these methods can be continuous wave (CW) light, time-resolved (TR) light, intensity modulated light or any combination of the above. In addition, the methods can be performed dynamically as function of time, and the image can be co-registered with an image obtained by magnetic resonance or computed tomography imaging. The multipoint incident illumination array (or detector array) can include a fiducial, and wherein the fiducial is used to determine the spatial localization of the array on the object.

The invention also features a method of detecting a cellular abnormality in a patient by using molecular probes targeted to a particular cellular abnormality, e.g., associated with a disease such as cancer, a cardiovascular disease, AIDS, a neurodegenerative disease, an inflammatory disease, or an immunologic disease. The invention also features a method of assessing the effect of a compound on a specified molecular target by using a molecular probe that is activated by the molecular target, wherein the probe is contacted to the target, the target is imaged prior to and after contact with the molecular probe, and the corresponding images are compared, wherein a change in the molecular target indicates the compound is effective. For example, the specified molecular target can be a protease, and the compound can be a protease inhibitor.

A molecular probe is a probe that is targeted to a molecular structure, such as a cell-surface receptor or antigen, an enzyme within a cell, or a specific nucleic acid, e.g., DNA, to which the probe hybridizes. A fluorophore is an agent that fluoresces. A fluorochrome is an agent that fluoresces (e.g., a fluorophore) and has a color.

Unless otherwise defined, all technical and scientific terms used herein have the same meaning as commonly understood by one of ordinary skill in the art to which this invention belongs. Although suitable methods and materials for the practice or testing of the present

7

invention are described below, other methods and materials similar or equivalent to those described herein, which are well known in the art, can also be used. All publications, patent applications, patents, and other references mentioned herein are incorporated by reference in their entirety. In case of conflict, the present specification, including definitions, will control.

5   In addition, the materials, methods, and examples are illustrative only and not intended to be limiting.

The new methods and systems provide various advantages. For example, the new methods and systems provide for the first time the ability to detect a fluorochrome distribution in the absence of pre-calibration or otherwise correcting measurements in

10   addition to a combination of measurements obtained during imaging of the object of interest. Furthermore, the new methods and systems enable the ability to image fluorescence activation, e.g., by enzyme activation, in deep tissue and to provide localization and quantitation in three dimensions. In addition, the new methods provide non-invasive, molecular imaging to provide information at subcellular levels.

15   The impact of the new molecular imaging techniques is significant. First, the new methods and systems can provide insight into specific molecular abnormalities that form the basis of many diseases, e.g., up-regulated proteases, other enzymes, cell surface receptors, cyclins, cytokines or growth factors in cancer. Second, the new methods can be used to assess efficacy of novel targeted therapies at a molecular level, long before phenotypic

20   changes occur. This, in turn, is expected to have an impact in drug development, drug testing, and choosing appropriate therapies and therapy changes in a given patient. Third, the new molecular imaging/quantitation methods and systems potentially enable one to study the genesis of diseases in the intact microenvironment of living systems. Fourth, the new methods of fluorescence-mediated molecular tomographic imaging are useful for testing

25   novel drug delivery strategies. Fifth, the imaging methods allow one to gain three-dimensional information that is much faster to obtain than is currently possible with time consuming and labor intensive conventional, basic science techniques.

The new imaging systems and methods will have broad applications in a wide variety of novel biologic, immunologic, and molecular therapies designed to promote the control and

30   eradication of numerous different diseases including cancer, cardiovascular, neurodegenerative, inflammatory, infectious, and other diseases. Furthermore, the described

8

detection systems and methods will have broad applications for seamless disease detection and treatment in combined settings.

Other features and advantages of the invention will be apparent from the following detailed description, and from the claims.

5

DESCRIPTION OF THE DRAWINGS

FIGs. 1A and 1B are examples of auto-quenched, activatable, near-infrared (NIR) fluorescent probes particularly suited for use in the new methods.

FIG. 2A is a schematic of a new three-dimensional, fluorescence tomography apparatus.

10   FIG. 2B is a schematic diagram of a positioning device used in conjunction with the apparatus of FIG. 2A to hold an animal in proper position for imaging.

FIG. 2C is a picture of an optical imaging chamber of the system of FIG.2A. The imaging chamber positions the source and detector fibers.

FIGs. 2D and 2E are alternative embodiments of fiber-coupling systems that can be

15   used in the new fluorescence tomography apparatus.

FIGs. 3A to 3F are a series of schematic diagrams of alternative embodiments of multipoint incident light arrays including circular arrays (as also shown in FIG. 2A), planar arrays, curved arrays, molded arrays, belt arrays, and catheter arrays. All of these embodiments can be used with the system shown in FIG. 2A.

20   FIG. 4A is a schematic of a time-resolved, three-dimensional fluorescence-mediated molecular tomography (FMT) system that can be used in conjunction with the system of FIG. 2A.

FIGs. 4B-4D are a series of photos of a positional insert used in the imaging chamber of the system of FIG. 2A (as shown in FIG. 4B), in a magnetic resonance imaging MRI coil

25   (FIG. 4C), and holding a mouse in an MRI coil (FIG. 4D).

FIG. 5 is flow chart of the steps used to process analog fluorescent and intrinsic (absorption) signal data in three dimensions to provide (i) a vector U of concentrations of activated fluorescent probes within a given volume, (ii) a vector D of concentrations of non-activated and activated probes, and (iii) a vector AR which is the ratio of activated over total

30   NIRF probe.

9

FIGs 6A-6C are a series of images representing an absorption map (6A), a fluorescence map (6B), and a molecular map showing the absorption ratio (AR).

FIGs. 7A and 7B are schematic diagrams illustrating absorption imaging at high resolution. FIG. 7A shows the phantom setup, and FIG. 7B illustrates the reconstructed

5 image.

FIGs. 8A and 8B are schematic diagrams of the experimental setup to image enzyme activity in three dimensions in a tissue-like medium using a circular multipoint incident light array in cross-section (8A) and in three dimensions (8B).

FIGs. 8C-8F are still images of a time-lapse video made of the enzyme activity

10 observed in the experimental setup shown in FIG. 8A at 20 (8C), 50 (8D), 115(8E), and 200 (8F) minutes, respectively.

FIGs. 9A-9C are a series of images from a live mouse imaged at a cross-section through the region of an implanted human tumor. FIG. 9A is a T2-weighted MR image. FIG. 9B is a NIR fluorescence-mediated molecular tomography (FMT) image of the tumor

15 obtained 24 hours after intravenous injection of an activatable cathepsin B-reporting NIR imaging probe. FIG. 9C is a fused image that demonstrates the good co-registration of the tumor as seen on the T2-weighted MR image and on the NIRF-activated FMT image.

FIGs 10A and 10B are a pair of images, MR and FMT, respectively, from a live mouse imaged at a cross-section at the level of the heart.

20 FIGs. 11A and 11B are a pair of images, MR and FMT, respectively, from a live mouse imaged at a cross-section at the level of the kidney.

Like reference symbols in the various drawings indicate like elements.

DETAILED DESCRIPTION

This invention relates to extracting quantitative molecular information from living

25 mammals and patients using fluorochromes, e.g., activatable fluorochromes, and a novel optical tomographic imaging method. This fluorescence-mediated molecular tomographic (FMT) imaging system is specifically designed to detect fluorescence, such as NIR fluorescence (NIRF), activation in deep tissues with high sensitivity, quantitatively and over time. High imaging accuracy and experimental simplicity are obtained because in one

30 embodiment only measurements acquired during imaging of the tissue of interest are used to

10

reconstruct the absolute optical properties associated with the fluorochrome distribution, e.g., fluorochrome concentration and/or lifetime. The system can use activatable NIRF molecular probes that are quenched and do not fluoresce until activated, or highly sensitive targeted NIRF molecular probes. The activatable molecular fluorochrome probes add molecular
5   specificity and yield high fluorescence contrast, to allow early detection and molecular target assessment of cancers and other diseased tissue in vivo. The systems include various components for obtaining the image data and one or more processors that include new algorithms to process the data to provide high levels of information and resolution.

The FMT imaging methods and systems enable extraction of molecular information
10   from diseased tissue. Thus, the systems and methods can be used to detect many molecular aberrations, as they occur in cancer, cardiovascular disease, inflammation, immunological diseases, arthritis, cutaneous and ophthalmic diseases, and others.

After reviewing the suitable probes and the general methodology of optical imaging, we will describe the new imaging systems and the processing required to obtain useful three-
15   dimensional, quantitative information.

Activatable NIR Fluorescent Probes

A fundamental paradigm shift in injectable contrast agents has recently been introduced by synthesizing probes that become brightly fluorescent following conversion by
20   specific enzymes (Weissleder et al., Nat. Biotechnol., 17:375-378, 1999) or become fluorescent by DNA hybridization (Tyagi et al., Nat. Biotechnol., 14:303-308, 1996). In their native state the probes are quenched either by a small molecule quencher (e.g., DABCYL (a non-fluorescent chromophore that serves as a universal quencher for any fluorophore in a molecular beacon: 4-(4-dimethylaminophenylazo)-benzoic acid) or QSY-7) or by multiple
25   fluorochromes (e.g., through energy resonance transfer). FIGs. 1A and 1B show schematics of two probes designed to target a specific enzyme (1A) and a specific DNA sequence (1B). When the fluorochrome is released or spatially separated from its quencher, fluorescence can increase up to 1000 fold. Because the spatial rearrangement of the quenched fluorochromes occurs only after specific interactions, these probes can be used to extract molecular
30   information from living organism. These activatable probes have four major advantages over other methods when single fluorochromes are attached to affinity molecules: (1) a single

11

enzyme can cleave multiple fluorochromes, thus resulting in one form of signal amplification, (2) reduction of background "noise" by several orders of magnitude is possible, (3) very specific enzyme activities can potentially be interrogated, and (4) multiple probes can be arranged on delivery systems to simultaneously probe for a spectrum of

5   enzymes.

A panel of highly specific enzyme-sensitive molecular probes have been synthesized that target matrix metalloproteinase-2 (MMP-2), cathepsin B/H, cathepsin D, cathepsin K, PSA, and caspase-3), and which are capable of fluorescence activation at 600-900 nm. These probes are described in detail in Weissleder et al., U.S. Patent No. 6,083,486; Weissleder et

10   al., Nat. Biotechnol., 17:375 (1999); Tung et al., Cancer Research, 60:4953-8, 2000; and Tung et al., Bioconj. Chem., 10:892-896, 1999). The activatable sensitive probes typically consist of three building blocks: (1) reporter fluorochromes, (2) target substrate, and (3) a delivery vehicle.

Reporter fluorochromes: Hundreds of optical probes have been developed for

15   microscopy and photodynamic therapy. Of these, fluorescent probes (i.e., excitation at shorter wavelength and emission at longer wavelength) are ideally suited for studying biological phenomena, as has been done extensively in fluorescence microscopy. If fluorescent probes are to be used in living systems, the choice is generally limited to the near infrared spectrum (600-1000 nm) to maximize tissue penetration by minimizing absorption

20   by physiologically abundant absorbers such as hemoglobin (< 550 nm) or water (> 1200 nm). Ideally the fluorochromes are designed to emit at 800 ± 50 nm. A variety of NIRF molecules have been described and/or are commercially available, including: Cy5.5 (Amersham, Arlington Heights, IL); NIR-1 (Dojindo, Kumamoto, Japan); IRD382 (LI-COR, Lincoln, NE); La Jolla Blue (Diatron, Miami, FL); ICG (Akorn, Lincolnshire, IL); and ICG

25   derivatives (Serb Labs, Paris, France). NIRF probes for in vivo use ideally should have the following properties: (1) narrow emission bandwidths, (2) high fluorescence efficiency (quantum yield), (3) biocompatibility, and (4) spectrally separated absorption and excitation.

Target Substrates: The release and or availability of individual fluorochromes is determined by interaction of a target substrate with its target. A target substrate can, for

30   example, be a peptide sequence that is cleaved by enzymes (see Table 1 below), a phosphate

12

group which is transferred by certain kinases, or a hybridizing DNA sequence recognizing a specific complementary DNA motif (see FIG. 1B).

Table 1:　Examples of Peptide Substrates (dots indicate the cleavage site)

Protease target	Peptide sequence
Cathepsin D	GPIC(Et)F·FRLG
Cathepsin B	GRR·G
Matrix metalloproteinase 2	GPLG·VRG
Caspase 3	DEVD·G
Prostate specific antigen	HSSKLQ·G

5

Delivery Vehicle: For a quenched probe to reach its intended target, it has to evade rapid clearance/elimination and overcome several structural barriers to delivery. These barriers include: (1) extravasation from vessels, (2) diffusion through tissue, and (3) cell membrane translocation in the case of intracellular enzymes (not required for secreted

10　enzymes). These barriers to delivery are fairly well investigated, and delivery vehicles can be selected using standard techniques and information. Suitable vehicles to deliver fluorochromes and substrates to a target, e.g., a tumor, in the body can be selected from a group of polymers, including protected graft co-polymers (Marecos et al., Bioconjug. Chem., 9:184-191, 1998) containing polyethylene glycol (PEG), polaxamers, and/or carbohydrates.

15　Additional delivery vehicles include dendrimers, proteins, carbohydrates, lipid spheres (e.g., emulsions, liposomes, and lipid self-assemblies), nanoparticles, and other materials commonly used for parenteral drug delivery.

Specific probes based on the above design for use in the new methods can be prepared as described in detail in Weissleder et al., U.S. Patent No. 6,083,486; Weissleder et

20　al., Nat. Biotechnol., 17:375-8, 1999; and Tung et al., Bioconj. Chem., 10:892-896, 1999.

One specific example of enzyme activatable probes for use in the new methods can be prepared as follows (see, Weissleder et al., U.S. Patent No. 6,083,486; Weissleder et al., Nat. Biotechnol., 17:375-8, 1999). A protected graft copolymer (PGC) consisting of a poly-L-lysine (PL) backbone and methoxy poly-e-ethylene glycol (MPEG) side chains is first

25　synthesized (Bogdanov et al., J. Drug Targeting, 4:321-330, 1997). In one example, Cy5.5 (absorption = 675 nm, emission = 694 nm, Amersham, Arlington Heights, IL) can be directly

13

attached to the poly-lysine backbone, yielding an activatable probe that can be cleaved by
cathepsin B/H and trypsin and has been used for the experiments described below. Briefly,
an excess of monoactivated Cy5.5 was reacted with PGC at pH 8.0 to yield the probe. The
final products were separated from free dye by size-exclusion chromatography. Trypsin and

5   cathepsin B/H-like proteases are capable of cleaving such probes as occasional free lysine
residues represent an enzyme substrate.

Alternatively, one can attach specific peptides conferring enzyme specificity directly
to the PGC. For example, cathepsin D sensitive probes have been synthesized (Tung et al.,
Cancer Res., 60: 4953-8, 2000 and Tung et al., Bioconj. Chem., 10:892-896, 1999). Briefly,

10   PGC was reacted with large excess of iodoacetyl anhydride to convert all amino groups on
the polylysine backbone into iodol groups. The cathepsin D specific peptide,
GIC(Et)FFKK(Fitc)C was attached to the iodinated PGC through a thiol specific reaction.
Thereafter, Cy5.5 was attached to the N-terminus and the free lysine side chains of the
cathepsin D substrate peptide. The advantage of this design is twofold: (1) a high loading

15   capacity (due to the fact that all lysines can be modified), and (2) that the fluorochrome
spacer is readily accessible to enzymes, thus resulting in improved release kinetics and signal
recovery.

Other NIR Fluorescent Probes

20   The probes described above are specifically designed to become activated upon target
interaction, e.g., target enzyme interaction. Alternative probes that can be used in the new
detection methods include (1) probes that become deactivated (quenched) after target
interaction, (2) probes that change their quantum yield upon target interaction, (3) probes that
change their fluorescence lifetime after target interaction, (4) probes that change their

25   fluorescence spectrum after target interaction, (5) wavelength shifting beacons (Tyagi et al.,
Nat. Biotechnol., 18:1191-1196, 2000), (6) multicolor fluorescence probes (Tyagi et al., Nat.
Biotechnol., 16:49-53, 1998), (7) probes that have high binding affinity to targets, i.e., that
remain within a target region while non-specific probes are cleared from the body. Examples
of the latter probes include receptor-targeted NIR fluorochromes (Achilefu et al., Invest.

30   Radiol., 35:479-485, 2000) or antibody-targeted NIR fluorochromes (Ballou et al.,
Biotechnol. Prog., 13:649-658, 1997), (8) non-specific agents with compartmental

distribution, (9) quantum dots, and/or (10) any fluorescent molecules with effects on fluorochromes. Another group of suitable fluorescent probes are long lifetime lanthanide metal–ligand probes that will allow the use of gated detection, and further increased sensitivity.

5

General Methodology

The new systems can use a charge-coupled device (CCD) camera and lens system to obtain "tomographic measurements" from the periphery of a multipoint incident light array, such as a cylinder with numerous, spaced, light emitters, for three-dimensional optical scans.

10   Improvements in NIR image quality are related to the number of sources and detectors used. The advantage of CCD technology is that increasing the detector density does not require additions in the detection hardware, just additional optic fibers to create a bigger array.

Fluorescence-Mediated Molecular Tomography (FMT)

15   The tomographic methodology described herein is an improvement of the general category of tomography using diffracting sources (see, e.g., Kak and Slaney, "Principles of Computerized Tomographic Imaging," IEEE Press, New York, 1988, pp. 208-218). The technique uses measurements of light at multiple projections to obtain information of the optical contrast inside turbid media such as tissue. In brief, diffraction tomography segments

20   the volume under investigation into a number of discrete voxels, referred to as a "mesh." The analysis is divided into two steps. The first step is the "forward problem," in which a diffusion equation is used to describe the photon propagation into an assumed medium, e.g., tissue, and is used to predict the field detected from this medium. The second step is the "inverse problem," in which the optical properties of each voxel of the assumed medium are

25   updated to minimize the errors observed between the predicted and measured fields. There are several ways to calculate the forward problem (analytical and numerical solutions of the diffusion equation) and inverse problem (direct inversion, χ^2 - based fits, and algebraic reconstruction techniques). Here a numerical solution of the forward problem is used to generate the prediction vectors for the fluorescence and intrinsic signal measurements (See

30   also FIG. 5). Inversion is based on the relaxed algebraic reconstruction technique. Higher order solutions can be obtained if needed when a solution is fed back in the forward problem

15

to produce more accurate forward propagation models, and this process can be repeated
iteratively.

The new FMT imaging systems use one or more laser sources to detect specific
chromophores or fluorophores and the forward problem is calculated for the specific
wavelength(s) used. Laser diodes can be used as light sources since they produce adequate
power, are within FDA class I and class II limits, and are stable, wavelength-specific and
economical. Light is directed to and from tissue using fiber guides, as this allows flexibility
in the geometrical set-up. For optical coupling, the fibers have to be in contact with tissue.
Alternatively, matching fluid is used to eliminate reflections due to air-silica-tissue index of
refraction mismatch.

Three different light source-detection technologies exist. Any combination of them
can be used for FMT applications as described herein. The simplest is continuous wave
(CW) imaging. This technique uses light of constant intensity and measures either (1) the
signal due to a distribution of excited fluorophores or (2) the attenuation of light (due to
tissue absorption and scattering) employing multiple source-detector pairs. The technique is
technically relatively simple and usually offers the best signal-to-noise (SNR) characteristics.
However, it is not best suited for imaging of intrinsic tissue contrast since it usually
introduces significant cross-talk between the calculations and imaging of absorption and
scattering coefficients. On the other hand, if the background optical properties are known,
the method is well-suited for imaging fluorophore concentration in the steady-state. To
produce activation information, a combination of this technologically simple approach with a
technology richer in information content can be used to obtain a both fluorescence and
intrinsic contrast images. A specific design is described below, in which the light source is
switched from one light emitter to another on a multipoint array in series, so that only one
emitter is illuminated at a time.

A more elaborate approach is to use intensity modulated (IM) light at a single or at
multiple frequencies. With this method, modulated light attenuation and phase shifts,
relative to the incident light, can be measured for multiple source-detector pairs. Compared
to a CW measurement, which yields intensity attenuation, the IM technique offers two pieces
of information, i.e., intensity attenuation and phase shift per source-detector pair. Amplitude
and phase are usually uncorrelated measurements and can more efficiently resolve the

absorption and scattering coefficient of intrinsic contrast. In the fluorescence mode, the technique can image two sets of information, fluorophore concentration and fluorescence lifetime.

The third approach, the time-resolved (TR) technique, uses short pulses of light injected into the tissue. The technique resolves the distribution of times that the detected photons travel into the medium for multiple source-detector pairs. Time-resolved methods contain the highest information content per source-detector pair, comparable only to the IM method performed simultaneously at multiple frequencies. This can be easily explained when one considers that the Fourier transform of the time-resolved data yields information at multiple frequencies up to 1 GHz, including the continuous wave components ($f = 0$ MHz) used by the previous two methods. Therefore, the time-resolved method offers a CW component for direct comparison with the CW system, but also intensity attenuation and phase-shift measurements at multiple-frequencies (via the Fourier transform) that can image intrinsic absorption and scattering, and also fluorophore concentration and fluorescence lifetime.

A cost-efficient embodiment of the invention is described in detail below (see FIGs. 2A-2C and FIG. 4). In this embodiment, the bulk information is collected using economical, massively parallel CW measurements (~1000 channels) and highly specific information of absorption and scattering parameters are collected with a smaller array of time-domain source-detection channels (~50-100 channels). The time-domain information is used in three ways. The first is to independently quantify the average absorption and reduced scattering coefficient at the emission and excitation wavelength. The second is to implement time-domain measurements of intrinsic signal into the intrinsic reconstruction scheme by Fourier transforming the time-domain data, hence obtaining multiple-frequency readings. Since the tomographic problem is written in the frequency domain (with CW measurements having zero frequency) the addition of extra, higher frequency measurements is straightforward (just adding additional lines in the weight matrix constructed for the appropriate frequency, for both real and imaginary decompositions). The third use of the time domain system is to implement time-domain measurements of fluorescent signal into the fluorescent reconstruction scheme by Fourier transforming the time-domain data, and obtain information of the fluorescence lifetime of the NIRF probe. Due to the equivalency of signals detected

17

using pulsed light or intensity-modulated light at multiple frequencies via the Fourier transform, identical methods and systems can result when using intensity modulated light at multiple frequencies. A simplified approach is to use intensity modulated light at a few or a single frequency.

5

Fluorescence-Mediated Molecular Tomographic (FMT) Imaging Systems

The new imaging systems include an apparatus with various components used to generate digital signal data from analog fluorescence emitted from a patient or animal body, and a processor programmed with algorithms that can process the digital signal data into

10   useful images that provide diagnostic and prognostic information. The systems can also obtain measurements of the incident light after it propagates through the tissue and obtain information on the intrinsic contrast of the body being imaged.

Apparatus

15   Diffraction tomography differs from simple projection imaging in that it requires tissue transillumination at multiple projections. Therefore, the construction of an appropriate light guiding apparatus is fundamental to obtain molecular tomographic images using NIR light. In one embodiment, the system features a multipoint incident illumination array and a multipoint detector array, both incorporated into a single cylinder, to be placed around the

20   animal or patient body. One such apparatus is shown in FIG. 2A and FIG. 4. The two instruments can operate sequentially.

System 10 includes a continuous wave (CW) laser source 12. The laser 12 uses constant intensity light. Two wavelengths obtained from two different lasers can be used for imaging the intrinsic contrast before the administration of the NIRF probe. For imaging the

25   fluorochrome Cy 5.5, one wavelength is set to 673 nm (excitation wavelength) and the other to 694 nm (emission wavelength). Imaging at both wavelengths is necessary so that accurate forward models are created for the excitation field from the source to the fluorophore and for the emission field from the fluorophore to the detector. The other combination of wavelengths will target the fluorochrome ICG at 750 nm (excitation) and 800 nm (emission).

30   The two wavelengths are time-shared since the measurements are not very demanding in terms of time efficiency and are coupled through an optical attenuator 14 to a 1 x 32 optical

18

switch 16 (e.g., an optical switch from Dicon FiberOptics Irvine CA). The optical switch 16 directs light from laser 12 to any one of multiple (sixteen in this embodiment) source fibers 18. Alternatively, all fibers can be illuminated simultaneously, each at a different wavelength. The key is to be able to distinguish each point of illumination on the multipoint

5   incident illumination array 20.

In this embodiment, the multipoint incident illumination array 20 is located within a resin cylinder 15 (also referred to herein as an "imaging chamber"), with several rings of multiple source fibers 18 connected around the cylinder. In essence, cylinder 15 has numerous holes drilled into it in a series of "rings" at different levels of the cylinder and

10   perpendicular to the central axis. The holes can be equally spaced around the perimeter of the cylinder. The source fibers 18 pass through the holes in cylinder 15 and end flush with the inner wall. A multipoint detector array 21 is incorporated into the same cylinder 15, in the form of rings of detector fibers 22 interleaved (alternating) with the rings of the source fibers 18. Again, the cylinder has holes drilled for each detector fiber. This provides three-

15   dimensional volume coverage within the cylinder. Detector fibers 22 form the detector array 21 of cylinder 15, and, like the source fibers, end flush with the inner wall of the cylinder. In this first implementation, three rings of twelve detection fibers each are interleaved with two rings of sixteen source fibers each, each ring at 3 mm from the next, thus covering a total cylinder height of 1.2 cm.

20   Cylinder 15 (including multipoint incident illumination array 20 and multipoint detector array 21) can be filled with a liquid optical contact medium (e.g., Intralipid® or an emulsion of TiO_2 particles and appropriate amounts of an absorbing fluorophore or fluorochrome that simulate the optical properties of the tissue examined), which serves as the "coupling" fluid of diffuse photons from the surface of the animal body to the detection

25   fibers. The concentration of TiO_2 particles for the matching fluid and the resin cylinder will be such as to induce scattering properties comparable with the average reduced scattering coefficient of mice.

Fluorescent light collected by multipoint detector array 21 is fed through detector fibers 22 to a two-dimensional emitted fluorescent light array 24. The two-dimensional array

30   21 transmits the analog fluorescent light emitted from the body through a long-pass filter 25 (depending on the fluorochrome used) and to a CCD camera 26. The long-pass filter 25 will

19

be selected for the appropriate cut-off wavelength, similar as done for surface reflectance type on imaging systems (Mahmood, Radiology, 213:866-870, 1999). To image intrinsic contrast the filter is removed. The CCD camera 26 is mounted on a breadboard, and a lens 27, or a system of macro lenses, images the two-dimensional emitted fluorescent light array
5   onto the CCD camera.

Optimum light attenuation will be set by the optical attenuator 14 so that measurements will not saturate the CCD camera. For a typical 16-bit CCD camera the useful dynamic range is approximately three to four orders of magnitude. This is also the dynamic range expected for measurements of diffuse light in small animals with body diameters of
10   about 2-3 cm. The dynamic range expected for human patients may differ depending on the target organ. For example, for human breast imaging, at an approximate diameter of 8 cm, the dynamic range required is about 6-8 orders of magnitude. This dynamic range can be covered using CCD technology by rapidly acquiring multiple frames. With current CCD technology used at 10 frames per second, the dynamic range can be 6 orders of magnitude in
15   one second of acquisition. For brain measurements, higher dynamic range may be achieved with longer acquisition times or more time-efficiency by using programmable attenuators that selectively attenuate the higher signals with a known level of attenuation.

Additionally a positional device 23 can be used for optimum placement of the animal in cylinder 15 as shown in FIG. 2B. The positional device in this embodiment is simply a
20   cylinder that fits snuggly within cylinder 15. Three positional devices 23 (cylindrical inserts) have been constructed. The first insert is constructed of Lexan® (polycarbonate) or Plexiglas®, and the second is constructed of white Delrin®, Polypropylene, or Kel-F®. Both of these inserts have an outer diameter that exactly fits the inner diameter of cylinder 20, 21, and are 1mm in thickness. The third insert is constructed out of Mylar® film and Kel-F®
25   film to produce an insert with a wall thickness of 0.1 mm diameter. The advantages of this design are that the animal is stabilized during imaging and that positional accuracy with surface marks can be established for co-registration purposes.

A detailed view of cylinder 15 (the imaging chamber), including both the multipoint detector array 21 and the multipoint incident illumination array 20, is shown in FIG. 2C. The
30   source fibers 18 and detector fibers 22 are arranged so that measurements are obtained along

20

the entire cylinder to allow for three-dimensional reconstructions. Source fibers 18 are interleaved between the detector fibers.

FIGs. 2D and 2E illustrate two alternative fiber-coupling systems. FIG. 2D shows the system used in FIG. 2A, in that a separate two-dimensional emitted fluorescent light array 24 is used to collect the signals of all detector fibers 22 in one plane, which is imaged by CCD camera 26 through filter 25. FIG. 2E shows a simpler embodiment in which the detector fibers 22 are directly connected to filter 25, i.e., filter 25 serves as the two-dimensional array 24.

Other embodiments of the multipoint incident illumination array are shown in FIGs 3A to 3F. FIG. 3A illustrates a top view of the cylindrical array described above. FIG. 3B shows a planar array used for reflectance and/or transmittance mode operation. In an alternative embodiment, the array is a portion of a cylinder, e.g., in the form of a curve with a set radius as shown in FIG. 3C. On the other hand, FIG. 3D shows a schematic of a molded array, in which the ends of the light source fibers are arranged on a rigid substrate that conforms to a specific shape of a body, or are arranged on a substrate of bendable, elastic material, such as a plastic, rubber, or cloth that can secure the light emitting optic fibers, and that can be molded to conform to a body shape. FIG. 3E illustrates a belt-like, uneven array, in which the ends of the source fibers are arranged in a flexible belt that can be fastened around a patient or the limb of a patient as required. The exact positions of the light emitting points within this array can be determined and corrected for by concomitant CT, US, or MR imaging. In an alternative embodiment, the ends of the light source fibers are provided in a catheter-like device as shown in FIG. 3F.

In each of these embodiments, the ends of the detector fibers 22 can be interleaved with the ends of the source fibers 18 as in the cylinder 15 shown in FIG. 2A. Alternatively, the detector array can be separate and distinct from the incident illumination array, as long as the ends of the detector fibers are spaced in a specified geometry with respect to the ends of the source fibers. For example, in the catheter-like array, the preferred mode of use is with a separate detector array that positions the ends of the detector fibers on the outside of the body while the incident light array is positioned inside the body, e.g., to image the prostate gland, lungs, vasculature, or gastrointestinal tract.

21

The apparatus 10 of FIG. 2A is used with a processor 11, e.g., located in a PC, as described in further detail below. As shown in FIG. 4, such a processor 11 generally includes an input/control device 60, a memory 62, and an output device 64. The processor 11 can be an electronic circuit comprising one or more components. The processor can be
5   implemented in digital circuitry, analog circuitry, or both, it can be implemented in software, or may be an integrated state machine, or a hybrid thereof. Input/control device 60 can be a keyboard or other conventional device, and the output device 64 can be a cathode ray tube (CRT), other video display, printer, or other image display system. Memory 62 can be electronic (e.g., solid state), magnetic, or optical. The memory can be stored on an optical
10   disk (e.g., a CD), an electromagnetic hard or floppy disk, or a combination thereof.

A highly efficient photon collection apparatus of FIG. 2A can be built using the same or similar components as discussed above, but with the exception that dedicated detector fibers 22 are directly coupled to the CCD (as shown in FIG. 2E), versus the lens system shown in FIGs. 2A and 2D. Overall, this system design should provide at least 300%
15   improved photon counting efficiency. Higher efficiency CCD chips will further improve photon detection.

To achieve a higher image-resolution design the apparatus of FIG 2A can accommodate more source-detector pairs (for example 64 x 100) either by a lens-imaging system (FIGs. 2A and 2D) or by direct coupling (as shown in FIG. 2E). The latter system
20   could require a larger dimension chip CCD camera to accommodate the larger detector set.

In use, baseline measurements can be obtained from the tissue at the excitation wavelength and at the emission wavelength without using the filter. Fluorescence measurements can be performed at the emission wavelength after inserting the appropriate cut-off filter.

25   An add-on system that will significantly enhance the tomographic accuracy is shown in FIG. 4A. This is a time-resolved FMT imaging system 30. A 16 x 16 channel array is implemented together with CW measurements to yield superior reconstructions. The CW and TR system can be used independently but a benefit is achieved when the measurements obtained from both systems are combined in the same reconstruction scheme.

30   In general, system 30 includes a pulsed laser source 32, a wavelength coupler 34 and a wavelength splitter 36. Two sets of two pulsed laser diodes (pulse width ~70 picosecond,

22

average power ~150 μW) are employed at the same wavelengths as the proposed CW system of FIG. 2A. The wavelengths are used time-multiplexed with 10 nm delays; they are detected simultaneously by the 16-channel single photon counting time-resolved system 44 (e.g., a SPC-600® from Pico-Quant, Berlin, Germany). The time-resolved system can share

5   the same source fibers 18' as the CW system 18 (by connecting both CW and TR light sources to the optical switch) or use separate, dedicated source fibers. The time-resolved (TR) detection fibers 22' will be interlaced with the CW detector fibers 22. The TR acquisition will be obtained at different times than the CW acquisition to avoid cross-talk between the CW and TR systems. The relatively small source-detector array 18', 22' of the

10   TR system (which can also be incorporated into cylinder 15) is capable of producing useful diffuse images. However, the two main contributions of the TR data will be (1) their simultaneous implementation is the inversions of Eq. 1 to obtain multi-frequency information in addition with the CW data offering a stand-alone CW-TR tomographer, but also (2) their use with the concurrent magnetic resonance (MR) information to obtain measurements of

15   fluorescence concentration and lifetime from the tumor lesions as identified on the MR images.

The pulsed laser source 32 produces laser light that is coupled by wavelength coupler 34 and then split by splitter 36. The splitter directs ~99% of the laser light along path 39a into the optical switch 16 and 1% of the light along path 39b into the detector module 40 via

20   the corresponding attenuators 38a and 38b. The light traveling along path 39b from attenuator 38b provides a "reference signal" that is used to monitor the system's temporal drifts and signal stability. The 99% part of the laser light on path 39a that is directed to the optical switch 16 is switched in the same manner as in the CW system to selected sixteen (or more, if needed) CW source fibers 18. There is no need to use two different switches and

25   source fibers. The same optical system used for the CW system can be used to also direct the photon pulses onto the tissue of investigation in the light chamber 15. Fibers 18 can be (but need not be) physically identical to fibers 18' and the only differentiation is made for ease of illustration to indicate their operation passing CW or TR signals. A 2-to-1 optical switch 16', e.g., provided within the Dicon switch 16, can select between the CW or TR source.

30   However, an independent TR detector fiber array (sixteen fibers) is required to direct the collected photons at the time resolved detection system 44. Cylinder 15 is the same as in

FIG. 2A. Fluorescent or intrinsic light emitted from the body is passed to the TR system as in FIG. 2A and to detector module 40. Fibers 22 indicate the detector fibers of the CW system shown on FIG 2A.

Detector module 40 includes photomutiplier tubes (PMT) 41 that detect photons and
5   convert single photons to electrical analog pulses. These analog pulses pass to router 42, which directs the pulses via path 43 to the SPC-600 board 44. Here the pulses are converted to digital values that indicate the time of arrival (TOA) of each coming pulse relative to the trigger pulse on path 52 coming from laser 32. Each collected pulse generates in router 42 a digital address, which uniquely marks the detection channel from which this photon was
10   detected. This digital address is directed to the computer memory 62 via digital cable 45 and is used to store the TOA in the appropriate memory bin allocated for each individual channel. For the sixteen channels used in this embodiment, there are sixteen separate digital addresses corresponding to sixteen separate memory bins. Within system 44, constant fraction discriminator CFD 50 rejects pulses that have a very small amplitude and are probably due to
15   photo-electronic noise, the Time-to-Amplitude Converter (TAC) converts the time of pulse arrival to an analog amplitude value, and the Multi-Channel Analyzer (MCA) converts this analog amplitude to a digital value at high speed. The output 47 of system 44 is a digital value stored in the computer memory bin that corresponds to the address carried on cable 45.

Time-resolved measurements can be used independently to obtain average
20   background properties of the medium measured, an important input parameter for absorption, scattering, and fluorescence reconstructions. The combination of TR and CW measurements will produce more accurate forward problems for the intrinsic contrast and fluorescence reconstructions. Furthermore, the simultaneous use of CW and TR data will enhance the overall image quality and fidelity. Another alternative would be to use the time-resolved
25   data to produce low-resolution images of background intrinsic contrast and use this information to create more accurate forward problems for the CW reconstructions for each animal.

The CW and especially the TR information (or the IM information by consequence of the Fourier transform) can further be combined with MR imaging data to produce accurate
30   quantitative measures of fluorophore concentration and fluorescence lifetime measurements. Time-resolved or intensity-modulated methods would significantly open the spectrum to

24

differentiate the fluorescence decay of existing and novel fluorochromes distributed in tissue. The cyanine fluorochromes that are described above typically have decay times ranging from 1 to 20 ns. While this timescale is useful for many biophysical measurements, there are numerous instances where longer decay times are desirable. For instance, one may wish to
5   measure rotational motions of large proteins or membrane-bound proteins. Processes on the microsecond or even the millisecond timescale have been measured using phosphorescence, which displays decay times ranging from 100 ns to 10 μs. The long lifetimes of specific lanthanide metal–ligand probes will allow the use of gated detection, which could be employed to suppress interfering autofluorescence from biological samples and can thus
10 provide further increased sensitivity.

One attractive feature is to combine molecular maps derived from FMT imaging with anatomical tomographic images, e.g., those derived from magnetic resonance (MR), X-ray computed tomography (CT), ultrasound (US) or even single photon emission tomography (SPECT) or positron emission tomography (PET) imaging. In particular, the combination
15 with MRI or CT is preferable given the high spatial resolution of these imaging techniques. DOT imaging (absorption only) has already been combined with MR imaging (Ntziachristos et al., P.N.A.S., USA, 97:2767-72, 1999) while one of the examples in this application teaches how to combine FMT imaging with MRI. This combination with MRI will enable: (1) the validation of FMT imaging in vivo by direct comparison of the MR and optically
20 acquired images, (2) a direct comparison of cancer appearance and detection limits based on the anatomical images obtained by T2-weighed MR images, the Gd-enhancement pattern, and molecular activity as resolved with optical imaging, and (3) the implementation of MR structural and functional information as a priori information in the optical inversion scheme to obtain highly accurate measures of localized fluorophore concentration and lifetime. The
25 combination of MRI and FMT also improves quantitation accuracy of fluorophore concentration and lifetime. Overall, molecular probing will improve the detection accuracy and introduce the ability of molecular target assessment.

To avoid interference with the magnetic field, non-magnetic fiber bundles can be used to transport excitation and emission light to and from exciter/detection systems to the
30 patient. For human applications, available commercial or custom-built MRI coils available in any MR facility can be used. The MR coils can be coupled to one of the geometries

described in FIGs. 3A-3F depending on the application. To identify the exact position of the multi-point incident illumination array and detector arrays, coupled to the skin, MR or CT imaging itself can be used. Knowledge of the spatial location of source fiber ends and detector fiber ends on uneven surfaces improves optical reconstructions. The skin-coupled fibers as shown in, e.g., FIG. 3E, or internally placed fibers, e.g., endorectally using the array of FIG. 3F, can be detected by imaging if the arrays are constructed of materials that are uniquely detectable, e.g., materials that include microreference phantoms filled with magnetic/x-ray absorbing compounds, certain chemicals, or plastics. For example, to identify the position of the multipoint incident illumination array and detector array cylinder and the optical fibers on the MR images, small reference capillaries filled with water and $CuSO_4$ can be attached to the cylinder to appear as bright spots on the MR images.

FIGs. 4C and 4D are representations of a magnetic resonance (MR) coil 65 used for co-registration purposes. Coil 65 is specially built to accommodate the animal insert 23 shown in FIG. 2B. Two implementations are considered. In one embodiment, after FMT imaging is performed, insert 23 containing the animal is removed from the imaging chamber 15 and positioned within MR coil 65. One or more specially designed glass capillaries 66 (1 mm glass tubes filled with water and copper sulfate) are attached to insert 23 and enable the MR and FMT images to be co-registered. Such a fiducial marker is visible as a bright circular spot on the left side of the MR image in FIG. 8A (discussed below). FIG. 4D shows a mouse positioned within positioning insert 23, within MRI coil 65. The second embodiment has the coil built directly around imaging chamber 15 of FIG. 2A so that concurrent MR and FMT examinations can be performed.

Data Collection

Five sets of measurements M1-M5 for each of the TR and CW used are obtained as shown in the flowchart of FIG. 5. The M3 measurement can be theoretically constructed or derived by means of the M2 measurement and therefore its acquisition be eliminated. Although subsets of the collected data can be used depending on the requirements of the application, the highest accuracy is obtained when the M1, M2, M4 sets are utilized for fluorochrome reconstructions and the M1, M2, M4, M5 sets are used for deriving optical maps.

As shown in FIG. 5, there are five sets of simple measurements (M1, 71; M2, 72; M3, 73; M4, 74; and M5, 75) to be obtained in initial step 70. In the first step 71, the fluorescence measurement M1, is obtained. This is a measurement where the source is scanned at multiple positions, and the detector acquires the light emitted from the tissue with the band-pass filter on, so that only the emission wavelength (fluorescence) is collected. In step 72, the second measurement, M2, is made as in step 71, but without the band-pass filter to acquire the intrinsic signal from the tissue at each wavelength. If the fluorescence signal is very small compared to the intrinsic signal no filter is required. However, if the fluorescence (M1) from the tissue of investigation is more than 1% of M2, then a cut-off filter is used to reject the fluorescence wavelength. In step 73, measurement M3 is made to acquire the amount of intrinsic light that passes through the fluorescence filter (high-pass filter) used in step 71. To achieve this measurement, the tissue to be investigated is removed from the cylinder, and a measurement is made from the matching fluid with the fluorescence filter (band-pass filter) on. This measurement is also used to acquire the contribution of ambient light and other photonic and electronic noise on a per source basis.

In another approach, the experimental measurement of M3 is circumvented and substituted by a constructed measurement M3 = q1(r) x M2 + ct, where q1 is the filter attenuation of the intrinsic field and is a spatially dependent factor that could account for radially dependent filter anisotropy. The factor q1(r) can be determined experimentally by flat field measurements or can be calculated based of filter specifications. Constant ct represents an image of the background dark noise measurement of the CCD camera. In addition, M3 can be written as M3 = q1(r) x M2' + ct, where M2' is theoretically calculated using a solution of the transport equation or an approximation of this equation such as the diffusion equation for a homogeneous medium with the average optical properties of the medium of investigation or for a heterogeneous medium obtained by using known information.

In step 74, measurement M4 is obtained with all sources turned off to acquire only the ambient (background) light and CCD noise. In step 75, measurement M5 is obtained without a filter and without tissue at the excitation and the emission wavelength using appropriate laser diodes. This measurement acquires the background signal.

27

Practically, for CW measurements each of measurements M1, M2, M3, and M5 is a series of Ns images (where Ns is the number of sources used). M4 is a single image of background noise. For the TR or IM light sources, each of M1, M2, M3, and M5, is a set Ns x Nd, where Nd is the number of detectors. For multispectral imaging the number of measurements acquired is multiplied by the corresponding number of wavelengths employed.

Composite Measurements (CM)

These simple measurements are combined to create self-calibrated (or composite) measurements of fluorescence M (step 80a) and intrinsic contrast M' (step 80b), i.e:

$$M = (M1 - M3)/(M2 - M4) \qquad\qquad \text{Eq. 1}$$

And

$$M' = \log((M2 - M4)/(M5 - M4) \qquad\qquad \text{Eq. 2}$$

Although not explicit in the above equation, the measurements M1-M5 are functions of the frequency. Therefore, CW and TR data (after Fourier transformation) are handled in exactly the same way. The rationale for this construction is that these composite measurement vectors are independent of instrumental gain variation, such as differences in the attenuation between different source or detector fibers and inhomogeneities within the CCD chip. Furthermore, these vectors subtract from the actual measurements systematic errors such as background noise (M4) or high-pass filter imperfectness (M3). Although several ways would exist to calibrate the measurements, these particular constructions are directed after the theoretical predictions of fluorescent and intrinsic signals, which is a necessary step for quantitative reconstructions. This point is elucidated in the following paragraph.

Depending on the specific application, other alternatives can be used to construct self-calibrated composite measurements. For example in dynamic imaging, where the fluorophore concentration and activation is monitored as a function of time, measurement M5 could be substituted by measurement M2 at time 0, preferably before the NIRF probe has been administered to the animal. Therefore the fluorochrome absorption can be accurately monitored as a difference signal from intrinsic tissue absorption.

28

Construction of the Forward Problem

To perform tomographic measurements a theoretical prediction of our composite
measurements (CM) (i.e., the measurement M and the measurement M') is required, which is

5   referred to as the "forward predictor" (P) or the "weight matrix." The P and CM are
combined to produce molecular tomographic measurements as described in the following
section. Herein the specific theoretical constructions that adapt tomographic principles of
diffraction tomography (Kak & Slaney 1988) are presented.

The P for fluorescence is constructed based on a modified Born prediction of the

10   forward problem (Ntziachristos V, Weissleder R, Opt. Lett., 26(12): 893-895, 2001).
Generally, the medium is assumed to contain a weakly absorbing distribution of
fluorophores. The fluorophores are excited by this photon distribution and act as a secondary
point source of fluorescent light. The fluorophores as two-level quantum systems and
saturation effects are ignored because of the small concentration of NIRF probes that are

15   administered. Then the standard Born expansion for fluorescence measurements can be
written as:

$$\phi_{fl}(\vec{r}_d,\vec{r}_s) = \int_V g_{fl}(\vec{r}-\vec{r}_d)\frac{\sigma c N_f(\vec{r})}{1-i\omega\tau}\phi_0(\vec{r},\vec{r}_s)d\vec{r} \qquad\qquad \text{Eq. 3}$$

20   where $\phi_{fl}(\vec{r}_d,\vec{r}_s)$ is the detected fluorescence fluence at position $\vec{r}_d$ for a source at

position $\vec{r}_s$, $\phi_0(\vec{r},\vec{r}_s)$ is the established photon fluence in the homogeneous medium due to a

source at position, and $g_{fl}(\vec{r}-\vec{r}_d)$ is a function that describes the propagation of photons in

the diffuse medium at the emission wavelength. $N_f(\vec{r}) = [F]\cdot\gamma$ is the unknown concentration

of the fluorophore F multiplied by the fluorescent yield γ at a position $\vec{r}$, σ is the absorption

25   cross-section of the fluorochrome, c is the speed of light in the diffuse medium, $\tau = 1/\Gamma$ is the

fluorescent lifetime and ω is the modulation frequency of the source light intensity. For

sources of constant intensity $\omega = 0$. Our construction of the forward predictor (P) in step 88,

which predicts measurement M (step 80a) is:

$$M = \frac{M1 - M3}{M2 - M4} = \frac{1}{\phi_0(\vec{r}_d, \vec{r}_s)} \int g_{fl}(\vec{r} - \vec{r}_d) \frac{ocN_t(\vec{r})}{1 - i\omega\tau} \phi_0(\vec{r}, \vec{r}_s) d\vec{r} \qquad \text{Eq. 4}$$

This is a modified Born expansion that normalizes the standard Born expansion
with the incident field $\phi_0(\vec{r}_d, \vec{r}_s)$. Therefore, the gain of sources and detectors are canceled
5   out for each source-detector pair independently.

For intrinsic contrast reconstructions, the forward predictor P' is determined (in step
88) using the Rytov expansion in the frequency domain, as described, e.g., in O'Leary et al.,
Opt. Lett. 20:426-428, 1995; and Ntziachristos et al., Proc. Natl. Acad. Sci., USA, 97:2767-
72 2000. Then the measurement M' (step 80b) can be written as:

10

$$M' = \log \frac{M2 - M4}{M5 - M4} = \frac{1}{\phi_0(\vec{r}_d, \vec{r}_s)} \int g_0(\vec{r} - \vec{r}_d) o(\vec{r}) \phi_0(\vec{r}, \vec{r}_s) d\vec{r} \qquad \text{Eq. 5}$$

where $\phi_0(\vec{r}, \vec{r}_s)$ is the incident field from the source at position $\vec{r}_s$ to position $\vec{r}$ and
$o(\vec{r})$ is the vector of the unknown absorption and diffusion coefficients changes relative to
the assumed homogeneous background medium.

15   The functions g_{fl} and ϕ_0 are calculated by simulating photon propagation at the
emission (step 82) and excitation (step 84) wavelengths for the specific imaging chamber
geometry and diffusion theory. This can be achieved either analytically or numerically. To
perform these simulations, knowledge of the tissue average optical properties in the
wavelengths of interest are required. The optical properties can be obtained by fitting all the
20   intrinsic contrast TR measurements to the diffusion model for the appropriate geometry.
Analytically, standard methods can be applied (adapted for the cylindrical geometry) as
described in Li et al., Appl. Opt., 36:2260-2272 (1997). Here however, we propose to use a
homemade finite-differences numerical algorithm that solves the diffusion approximation for
a cylindrical geometry using a partial boundary condition (Arridge, Inverse Problems,
25   15:R41-R93, 1999), which accurately models even small source-detector separations. This
must be used to obtain more accurate propagation models for the smaller scale problem. The
only unknown in Eq. 4 and Eq. 5 are then the distribution of the fluorophore or the

absorption and diffusion coefficients respectively. The minimization of Eqs. 4 and 5 is described in the next section.

Data Inversion

Both fluorescence and intrinsic contrast reconstructions are based on the creation of a function that is subsequently minimized. In step 80a the composite measurement M is used to construct the function $F(U) = (M - P \times U)^2$ and in step 80b the composite measurement M' is used to construct a function $F'(O) = (M' - P' \times O)^2$, where U is the vector of unknown non-quenched (activated) fluorochrome concentration and O is the vector of unknown absorption and diffusion distributions. The absorption distribution can be converted to flurochrome concentration via the Beer-Lambert Law. The matrices P, P' are described in the previous section. In steps 92a and 92b, the functions F(U) and F'(O) are minimized to obtain the distribution and magnitude of U and O, respectively. The minimization is obtained using algebraic reconstruction techniques although any other minimization method can me used to find the solution of the constructed functions.

Iteration is not necessary when only small amounts of fluorochrome are activated. This is the most typical case. However, if for certain applications large concentrations of activated fluorochrome are expected (namely the absorption perturbation yielding more than 10% variation in the intrinsic signal), then iterative steps are necessary. The first step of the iterative process 95 assumes a homogeneous background with the average optical properties of the medium of investigation. Subsequent steps use images U and O as background maps in the creation of matrices P, P'. When iteration is used, the creation of P, P' using numerical solutions of the diffusion equation is necessary. Iteration is also necessary when the background distribution of the fluorochrome is comparable to the contrast obtained from localized areas of high accumulation such as the tumor. Iteration is typically stopped when each iteration step does not significantly change the calculated result.

Molecular Maps

The new systems and methods enable the quantitative, three-dimensional calculation of molecular and molecular-activation maps. The resolved image U contains the concentration of fluorescing or activated fluorochrome, whereas the absorption image

31

contained in O is a quantitative representation of the total fluorochrome concentration (quenched and de-quenched). The ratio of activated over total fluorophore concentration is the activation ratio map (step 93):

$$AR = U/O \qquad\qquad Eq.\ 6$$

which represents the amount of activation normalized by the amount of fluorochrome actually distributed in the volume of investigation. For volumes in which the absorption is zero the ratio AR is not defined. This is natural, since for zero fluorochrome distribution there should be no activation. Therefore, the ratio AR is by default applied only in the volume elements with non-zero absorption.

The generation of a molecular map (reporting the activity of the enzyme tryspin) is shown in FIGs. 6A-6C. A molecular map is a representation of an endogenous process or molecule. A molecular map (MM) is best described as $MM = k * AR$, where k is a constant; i.e., $MM = k * (U/O)$.

FIG. 6A is an image of an absorption map, showing the concentration of a molecular probe sensitive to degradation by trypsin. The bright spot in FIG. 6A is a representation of the total amount of the probe, both the quenched and the unquenched fractions. FIG. 6B is the corresponding fluorescence map, which measures only the fraction of de-quenched (i.e., enzyme activated) trypsin sensitive probe. FIG. 6C provides the AR image, or "molecular map," displaying the "fluorescence activation" as an image where the bright spot is directly proportional to the amount of added trypsin enzyme used in this experiment.

EXAMPLES

The invention is further described in the following examples, which do not limit the scope of the invention described in the claims.

Example 1 – FMT Images of a Phantom

In one embodiment, phantom experiments were performed to verify the three-dimensional position and accuracy of measurements. The experimental set-up is illustrated in top view in FIG. 7A. Briefly, a phantom 100 containing 3 capillary tubes (1 mm internal

32

diameter) 103, was constructed using a triangular geometry and inserted into the optical chamber (15 in FIG. 2A) containing a turbid medium 102 (0.5% Intralipid® in water). The capillaries 103 were separated 8 and 11 mm from each other as shown in FIG. 7A, and were coated with a black fluorochrome to maximize absorption. The capillaries were imaged three dimensionally.

FIG. 7B depicts the reconstructed image 110 at a plane perpendicular to the longitudinal axis of the imaging chamber 15, at about the middle of the three-dimensional volume imaged. The high contrast allowed for high-resolution imaging of the three capillaries with high positional precision. The reconstruction mesh used was 0.8 x 0.8 x 2 mm^3. The reconstruction used 24 sources x 36 detectors.

Example 2 – FMT Images of Trypsin Activity Over Time

In another experiment, quantitative, spatially localized information on fluorescence activation was obtained as a function of time. As shown in FIGs. 8A and 8B, a 3mm tube 123 was immersed in a tissue-like fluid (Intralipid®) to form phantom 102. The tube contained 1.5 μM of a Cy5.5 probe, which was activated by the addition of the enzyme trypsin into the tube at time 0. Only a single plane was imaged in this experiment by sequentially illuminating each of twelve light emitting points in the direction of curved arrow 125. FIG. 8B illustrates the phantom in a three-quarter view.

FIGs. 8C to 8F illustrate a series of axially reconstructed frames obtained at different time points. The frames show the probe activation as a function of time. For example, as shown in FIG. 8C, at 20 minutes after trypsin was added to the capillary, only ~20% of the probe had been activated. However, as shown in FIG. 8F, at 200 minutes after the enzyme was added, ~75% of the probe had been activated. Each frame was acquired by sequentially directing light in each one of twelve source fibers located on the same plane along the cylinder. For each source, the CCD acquired light from the detector fibers for 5 seconds. The total acquisition time per frame was therefore 1 minute (12 sources x 5 seconds each).

Example 3 – Multiple Co-Registered Images of Cathepsin B Activity in a Mouse

In another experiment, combined MR/FMT imaging was used to obtain maps of cathepsin B protease activity in human tumors implanted in nude mice (FIGs. 9A-(C). The

tumors were cathepsin B rich HT1080 fibrosarcoma, which had been implanted into the mammary fat pad 7-10 days prior to the experiment. The animals received an IV injection of a cathepsin B sensitive imaging probe (Weissleder et al., Nat. Biotechnol., 17:375-378, 1999) at 24 hours prior to the imaging experiments. The animals were anaesthetized with an

5   intraperitoneal injection of 90 mg/kg ketamine and 9 mg/kg xylazine and were placed into the insert 23 shown in FIG. 2B. The insert and animal were placed into the imaging chamber 15 and measurements M1, M2, M3, and M4 were obtained.

Subsequently, the mouse within the insert was removed from the imaging chamber. Fiducials (as described herein) with water were attached to predetermined positions on the

10   periphery of the insert. The insert was subsequently placed in the MR coil and a set of axial T2-weighted imaged were obtained. The role of the fiducials was to identify on the MR images the position of selected source and detector fibers for later co-registration of the images. The fiducial (a glass capillary tube arranged longitudinally along the outside cylinder wall) shown on the slices of FIGs. 9A, 10A, and 11A as a bright spot on the left side

15   of the image, for example, indicates the position of detectors 1, 13, and 25 on the corresponding slices.

The results show an MR image (FIG. 9A), a cathepsin B molecular map (FMT)(FIG. 9B), and one of the MR slices fused with the FMT image to produce a combined MR/molecular map (FIG. 9C). There is excellent congruence of optical and MR contrast

20   from the images obtained at the tumor level. The tumor demonstrates strong molecular activity of cathepsin B (fluorescence activation), corroborated by immunohistochemsitry and Western blotting. The co-registration of the fluorescent activation and T2 image are shown on the fused image in FIG. 9C. The remaining two rows of images are slices that show cathepsin B absence and/or presence in other tissues. Specifically, FIGs. 10A and 10B show

25   an MR image and FMT image at heart level, respectively. As expected, there is no cathepsin B activity in the lung and heart, and thus nothing lights up on the FMT image in FIG. 10B. FIGs. 11A and B show an MR image and FMT image at kidney level, respectively. The fluorochrome appearing in the kidney is likely excreted excess, and does not reflect cathespin activity.

30   This is an example where a subset of the full measurement array is used (only M1 through M4 CW measurements, no M5 and no TR data) to produce a enzymatic activity

34

image that conveys useful information for the clinical examples describes in the following examples. Moreover, this series of images in FIGs. 9A to 11B confirms that the new methods and systems can be used to generate multi-slice images of living animals.

5   Example 4 – Molecular Maps

To demonstrate the use of producing molecular maps we have used the set-up of Example 3, but acquired the full array of M1 through M5 measurements in CW mode. The optical properties of Intralipid® were independently measured with a time-resolved system. Then a fluorescence map (FIG. 6B) collected 50 minutes after trypsin activation and an

10   absorption map (FIG. 6A) were constructed according to the algorithm described in the flowchart in FIG. 5. The molecular map (AR image) calculated according to step 93 is shown in FIG. 6C and demonstrates 40% activation of the enzyme sensitive probe 50 minutes after activation.

15   Example 5 – Enzyme-Specific Probes

We have synthesized a number of different sensitive enzyme-specific imaging probes useful for FMT imaging. The probes are specific for cathepsin D, cathepsin K, the enzymatically active form of prostate specific antigen (PSA), and matrix metalloprotease-2, among other enzymes. The specificity of these probes was shown by incubation with

20   purified or recombinant human enzymes and by measurement of fluorescence activation in a fluorometer. The NIR fluorophore Cy5.5 was used as a quenched reporter in all of these probes. Any of these probes can be used in animals and human patients as described herein to measure enzyme activity within deep tissues (both normal and diseased tissues). For example, MMP-2 activity can be measured in tumors before and after treatment with an

25   MMP-2 inhibitor (e.g., Prinomastat®, Agouron Pharmaceuticals, Inc., San Diego, CA). Such measurements of molecular target assessment are useful for rapid drug efficacy screening in vivo in animal models. Moreover, such screening methods can be used to assess the efficacy of a particular therapy in a specific patient.

30

Example 6 - Clinical Use

The new FMT methods are expected to have broad clinical implications. One use is for early detection of disease at a stage when molecular abnormalities are present, but have not yet led to phenotypic abnormalities (e.g., mutations in cancers which have not yet produced a tumor mass). Another use is for molecular target assessment in diseased tissues (1) to determine if a given target is present in a patient (e.g., level of expression of a protease), (2) to determine whether an experimental drug has an effect on its intended molecular target in vivo, (3) to individualize and tailor treatments for a given patient, and (4) to optimize the dose of a given molecular drug for a given patient. In this sense, the new FMT imaging methods are an adjunct to testing drug efficacy. Such measurements would also be of value in a clinical setting to determine the effects of enzyme inhibitor drugs, receptor blockers, and other molecular drugs. The methods could be used to monitor a wide variety of disease including cancer, cardiovascular disease, AIDS, infection, immunologic diseases, inflammation, dermatological and ophthalmic diseases, neurodegenerative disease and others.

Example 7 - Multiple Probes

The new FMT methods can be performed with the concomitant use of multiple molecular probes (each with their own, specific excitation and emission wavelengths) to report multiple molecular abnormalities during the same FMT imaging acquisition. The described system can be adapted by adding one or more new laser sources to excite the additional fluorescent molecular probes. Imaging signals are collected through appropriate filter systems, making sure that there is not spectral overlap among the different channels. Image reconstruction, algorithms, and displays are similar to those for single wavelength imaging described herein.

Example 8 - Frequency Domain Technology

The TR system described herein can be modified by using one or more frequency domain sources, preferably at multiple frequencies. The theoretical formulation is written in the frequency domain so that the use of frequency technology is directly applied to the existing algorithms. The rationale behind using frequency domain technology is similar to

36

TR technology in that it yields multi-frequency information that can differentiate absorption and scattering in intrinsic contrast mode and fluorophore concentration and life-time in fluorescence mode. If frequency technology is used, the instrument in FIG. 4A is substituted by sources modulated at one or several frequencies and detection channels that are

5   responsible for signal demodulation, such as lock-in amplifiers or preferably quadrature demodulators, similar to the ones used for the detection of MR signals.

Example 9 - Differential Dynamic Imaging (DDI)

The implementation of the composite measurements described above can be applied

10   in several ways to obtain fluorescent and intrinsic contrast, and to construct the AR images. For example, whereas a general scheme of an animal injected with a NIRF molecular probe is considered in Eqs. 4 and 5, one can obtain measurements from an animal before injection of the NIRF probe and then obtain differential measurements of absorption and fluorescent contrast after NIRF probe injection. This technique has important applications in monitoring

15   the kinetics of uptake and activation (as also demonstrated in Example 2). This approach also yields the most accurate results since differential measurements allow for the reconstruction of the fluorochrome/chromophore absorption independently of background absorption (since only the absorption change can be reconstructed). Therefore, more accurate AR maps can be produced as a function of time.

20

Example 10 - Imaging at Multiple Wavelengths

An alternative implementation of composite measurements than the one used in Example 9 is to employ four or more wavelengths for each measurement set. For N tissue chromophores, N or more of these wavelengths are selected at a spectral region where the

25   NIRF probe does not absorb. Therefore, true "intrinsic" contrast is obtained, i.e., contrast that is due only to the natural tissue chromophore concentrations. Using the spectral information of these chromophores, one can calculate their absorption at the emission and excitation wavelengths of the NIRF probe. The other two wavelengths are used to construct absorption images at the excitation and emission wavelengths. Those latter images

30   reconstruct absorption due to both the natural tissue chromophore concentration and the fluorochrome distribution. By subtracting the images obtained at the excitation or emission

37

wavelength from the absorption images calculated only for the tissue natural chromophores, one can obtain the true fluorochrome/chromophore concentration.

Example 11 - Clinical FMT System

5   The new systems and methods described herein are easily applied to a clinical setting. For example breast cancer detection can be achieved with a circular/cylindrical multipoint incident illumination array or with a compression/planar array. Brain measurements can be made with an elastic band of optical fibers attached to the skull or a planar/reflectance geometry could be applied. See FIGs. 3A-F for various arrays. The described FMT imaging

10   methods can be conducted sequentially or simultaneously with MR or CT measurements, because the optical technology is compatible with other radiological modalities.

In a clinical setting, CW measurements would be useful for the economical collection of large numbers of measurements. However, even a limited number of more advanced technologies (e.g., IM or TR as described above) can significantly improve the information

15   content of the CW measurements. However, it is envisaged that a clinical system can be built entirely based on CW technology. As frequency-domain or time-domain technologies become cheaper, the whole system can be based only on frequency-domain or time-domain technologies.

20   **OTHER EMBODIMENTS**

A subcategory of the general reconstruction scheme of molecular activation described is the use of simple transillumination of tissue for the detection of molecular events. This is a relaxation of the tomographic imaging to simple projection imaging, similar, but not same as the one described previously for reflectance imaging (Weissleder et al., U.S. Patent No.

25   6,083,486). Transillumination allows for measurements of absorbers of fluorochromes through the whole tissue, therefore it achieves penetration of several centimeters, in contrast to reflectance imaging, which can penetrate only for a few centimeters at the most. Transillumination of molecular events cannot resolve or quantify molecular activity in three dimensions, but can still be used to qualitatively monitor relative changes of molecular

30   activation.

In another embodiment, the new systems and methods can be used to image endogenous fluorescence in an animal. For example, a gene encoding a fluorescent protein, such as green fluorescent protein or fluorescein, can be included adjacent to a gene of interest that is to be expressed in an animal or human patient using standard gene therapy techniques. The expression of the gene of interest can be determined indirectly by imaging the fluorescent protein. If this protein is expressed, then the gene of interest has also been expressed.

It is to be understood that while the invention has been described in conjunction with the detailed description thereof, the foregoing description is intended to illustrate and not limit the scope of the invention, which is defined by the scope of the appended claims. Other aspects, advantages, and modifications are within the scope of the following claims.

WHAT IS CLAIMED IS:

1. A fluorescence-mediated molecular tomography (FMT) imaging system comprising

a light source to provide incident light;

a multipoint incident illumination array to direct light into an object from two or more separate excitation points;

multiple optic fibers to transmit light from the light source to each point in the multipoint incident illumination array;

a multipoint detection array to collect light emitted from the object from two or more separate collection points;

a two-dimensional emitted light array to transmit light emitted from the object to a detector;

multiple optic fibers to transmit light from each collection point to a corresponding point on the two-dimensional emitted light array; and

a detector to detect and convert light emitted from each point of the two-dimensional emitted light array into a digital signal corresponding to the light emitted from the object.

2. The system of claim 1, wherein the light source is a near-infrared (NIR) light source.

3. The system of claim 1, wherein the object is a human patient and the multipoint detection array is configured to fit onto a portion of the patient

4. The system of claim 1, wherein emitted light is fluorescent light.

5. The system of claim 1, wherein the emitted light is continuous wave (CW) light, time-resolved (TR) light, intensity modulated (IM) light, or any combination thereof.

6. The system of claim 1, further comprising a processor that processes the digital signal produced by the detector to provide an image on an output device.

7. The system of claim 6, wherein the output device provides multiple images simultaneously.

8. The system of claim 6, wherein the processor is programmed to process the digital signal by

i) generating a corrected fluorescence measurement by subtracting a background signal and filter bleed-through signal from collected fluorescence measurements;

ii) generating a corrected intrinsic diffuse signal by subtracting the collected background ambient light signal from a collected intrinsic signal; and

iii) generating a self-calibrated fluorescence measurement by dividing the corrected fluorescence measurement by the corrected intrinsic diffuse signal.

9. The system of claim 6, wherein the processor is programmed to process the digital signal by

i) generating a corrected fluorescence measurement by subtracting a background signal and filter bleed-through signal from collected fluorescence measurements;

ii) generating a corrected intrinsic signal measurement by subtracting a collected background ambient light signal from collected intrinsic signal measurements;

iii) generating a self-calibrated fluorescence measurement by dividing the corrected fluorescence measurement by the corrected intrinsic measurement;

iv) generating a corrected background-medium diffuse signal by subtracting the collected background ambient light signal from a collected diffuse signal; and

v) generating a self-calibrated intrinsic measurement by dividing the corrected intrinsic signal measurement by the corrected background-medium diffuse signal.

10. The system of claim 6, wherein the processor is programmed to process the digital signal by

i) generating a self-calibrated measurement $M = M1 - M3 / M2 - M4$, wherein M1 is an emission wavelength fluorescence signal, M2 is an intrinsic signal, M3 is a background bleed-through signal, and M4 is a background ambient light signal.

41

11. The system of claim 6, wherein the processor is programmed to process the digital signal by

i) generating a self-calibrated measurement $M = (M1 - (q1(r) \times M2 - ct)) / (M2 - M4)$, wherein M1 is an emission wavelength fluorescence signal, M2 is an intrinsic signal, M4 is a background ambient light signal, q1 is a filter attenuation of an intrinsic field, and ct is a constant that represents an image of background dark noise measurement.

12. The system of claim 6, wherein the processor is programmed to process the digital signal by

i) generating a self-calibrated measurement $M = M1 - M3 / M2 - M4$, wherein M1 is an emission wavelength fluorescence signal, M2 is an intrinsic signal, M3 is a background bleed-through signal, and M4 is a background ambient light signal; and

ii) minimizing a function $F(U)$ of $(M - P \times U)$ to obtain a distribution and magnitude of U, wherein U is a vector of unknown concentration of a target in the object being imaged and P is a forward predictor of M calculated by solving a diffusion equation for an appropriate geometry and background medium in fluorescence mode.

13. The system of claim 6, wherein the processor is programmed to process the digital signal by

i) generating a self-calibrated intrinsic measurement $M' = \log (M2 - M4)/(M5 - M4)$, wherein M2 is an intrinsic signal, M4 is a background ambient light signal, and M5 is a background-medium diffuse signal;

ii) minimizing a function $F'(O)$ of $(M' - P' \times O)$ to obtain a distribution and magnitude of O; wherein O is a vector of unknown concentration of a fluorophore in the object, and P' is a forward predictor of M' calculated by solving a diffusion equation for the appropriate geometry and background medium in absorption/scattering mode;

iii) calculating an activation ratio $AR = U/O$; and

iv) generating an image corresponding to AR.

14. The system of claim 6, wherein the processor is programmed to process the digital signal by

i) generating a self-calibrated measurement M = M1 – M3 / M2 – M4, wherein M1 is an emission wavelength fluorescence signal, M2 is an intrinsic signal, M3 is a background bleed-through signal, and M4 is a background ambient light signal;

ii) generating a self-calibrated intrinsic measurement M' = log (M2 – M4)/(M5 – M4), wherein M5 is a background-medium diffuse signal;

iii) minimizing a function $F(U) = (M – P \times U)^2$ to obtain a distribution and magnitude of U, wherein U is a vector of unknown concentration of a target in the object being imaged and P is a forward predictor of M calculated by solving a diffusion equation for an appropriate geometry and background medium in fluorescence mode;

iv) minimizing a function $F'(O) = (M' – P' \times O)^2$ to obtain a distribution and magnitude of O; wherein O is a vector of unknown concentration of a fluorophore in the object, and P' is a forward predictor of M' calculated by solving a diffusion equation for the appropriate geometry and background medium in absorption/scattering mode;

v) calculating an activation ratio AR = U/O; and

vi) generating an image corresponding to AR.

15. The system of claim 1, wherein the multipoint incident illumination array is a cylinder that comprises at least 12 points of light.

16. The system of claim 15, wherein the cylinder further comprises the multipoint detection array.

17. The imaging system of claim 1, wherein the multipoint incident illumination array is a belt that comprises at least 12 points of light.

18. The imaging system of claim 17, wherein the belt further comprises the multipoint detection array.

19. The imaging system of claim 1, wherein the multiple optic fibers to transmit light from each collection point of the detection array comprise more than 100 separate fibers, and wherein the detector array comprises at least 100 collection points.

20. The imaging system of claim 1, wherein the multipoint incident illumination array comprises a flat plate.

21. The imaging system of claim 1, wherein the multipoint incident illumination array comprises two flat plates spaced apart and arranged in parallel.

22. The imaging system of claim 1, wherein the two-dimensional emitted light array transmits to the detector a two-dimensional pattern of multiple points of light corresponding to light emitted from the patient in three-dimensions, wherein the pattern varies over time at a rate corresponding to switching of illumination from one to another of the two or more excitation points.

23. The imaging system of claim 1, wherein the two or more excitation points are illuminated by the light source one at a time.

24. The imaging system of claim 1, wherein the light directed into the object has a wavelength of from 550 to 950 nanometers.

25. The imaging system of claim 1, wherein the detector comprises a charge-coupled device (CCD) camera.

26. The imaging system of claim 1, wherein the detector comprises a photomultiplier tube.

27. The system of claim 1, further comprising NIR fluorescent (NIRF) molecular probes, activatable fluorescent probes, targeted fluorescent probes, or non-specific fluorescent probes.

28. The system of claim 27, wherein the NIRF probes are activatable molecular probes.

29. A method for displaying an optical molecular map corresponding to a ratio of (1) a concentration of a molecular probe comprising a fluorophore administered to a patient, and (2) a concentration of an activated fluorophore corresponding to a specific target in the patient, the method comprising:

i) providing a first data set of fluorophore concentration based on intrinsic absorption;

ii) providing a second data set of activated fluorophore concentration based on calibrated fluorescence;

iii) dividing the first data set by the second data set on a point-by-point basis to provide a third data set; and

iv) processing the third data set to provide an optical molecular map corresponding to a ratio of (1) a concentration of a molecular probe comprising a fluorophore, and (2) a concentration of an activated fluorophore corresponding to a specific target in the patient.

30. A method of obtaining a three-dimensional, quantitative, molecular tomographic image of a target region within a patient, the method comprising

administering a fluorescent molecular probe to the patient, wherein the molecular probe selectively accumulates within a target region in the patient;

directing light from multiple points into the patient;

detecting fluorescent light emitted from the patient; and

processing the detected light to provide a three-dimensional image that corresponds to the three-dimensional target region within the patient and to the quantity of molecular probe accumulated in the target region.

31. The method of claim 30, wherein the light is near-infrared (NIR) light, and the probe is a NIR fluorescent (NIRF) molecular probe.

32. The method of claim 30, wherein the three-dimensional image is visualized on a two-dimensional output device.

33. The method of claim 30, wherein the processing comprises digitizing the fluorescent signal emitted from the patient, self-calibrating the digital signal by combining

45

fluorescent and intrinsic signal measurements from the patient and background medium, and reconstructing a three-dimensional, quantitative image.

34. The method of claim 30, wherein the processing comprises

i) generating a corrected fluorescence measurement by subtracting a background signal and filter bleed-through signal from collected fluorescence measurements;

ii) generating a corrected intrinsic signal measurement by subtracting a background ambient light signal from collected intrinsic signal measurements;

iii) generating a self-calibrated fluorescence measurement by dividing the corrected fluorescence measurement by the corrected intrinsic measurement;

iv) generating a corrected background-medium diffuse signal by subtracting the collected background ambient light signal from a collected diffuse signal; and

v) generating a self-calibrated intrinsic measurement by dividing the corrected intrinsic signal measurement by the corrected background-medium diffuse signal.

35. The method of claim 30, wherein the processing comprises

i) generating a self-calibrated measurement $M = M1 - M3 / M2 - M4$, wherein M1 is an emission wavelength fluorescence signal, M2 is an intrinsic signal, M3 is a background bleed-through signal, M4 is a background ambient light signal;

ii) generating a self-calibrated measurement $M' = \log (M2 - M4)/(M5 - M4)$, wherein M5 is a background-medium diffuse signal;

iii) minimizing a function $F(U)$ of $(M - P \times U)$ to obtain a distribution and magnitude of U, wherein U is a vector of unknown concentration of a target in the object being imaged and P is a forward predictor of M calculated by solving a diffusion equation for an appropriate geometry and background medium in fluorescence mode;

iv) minimizing a function $F'(O)$ of $(M' - P' \times O)$ to obtain a distribution and magnitude of O; wherein O is a vector of unknown concentration of a fluorophore in the object, and P' is a forward predictor of M' calculated by solving a diffusion equation for the appropriate geometry and background medium in absorption/scattering mode;

v) calculating an activation ratio $AR = U/O$; and

vi) generating an image corresponding to AR.

46

36. The method of claim 30, wherein administering the molecular probe comprises systemically injecting an activatable molecular probe.

37. The method of claim 30, wherein administering the molecular probe comprises locally injecting an activatable molecular probe into the target region.

38. The method of claim 30, wherein administering the molecular probe comprises locally injecting an activatable molecular probe into a non-target region.

39. The method of claim 30, wherein the light directed into the patient is at a wavelength of from 550 to 950 nanometers.

40. The method of claim 30, wherein the light is directed into the patient from at least 32 separate points of light arranged in a fixed three-dimensional geometry.

41. The method of claim 30, wherein the light is directed into the patient with a multipoint incident illumination array comprising a belt having at least 12 points of light.

42. The method of claim 41, wherein the belt further comprises a multipoint detector array.

43. The method of claim 42, wherein the spatial localizations of the multipoint incident illumination array and the multipoint detector array are determined by image co-registration.

44. The method of claim 30, wherein fluorescent light emitted from the patient is detected by a charge-coupled device (CCD) camera from a two-dimensional emitted fluorescent light array.

45. The method of claim 44, wherein photon pulses are directed into the patient and the arrival of photons emitted from the patient is time-resolved using a separate array of photon detectors.

46. The method of claim 30, wherein the emitted light is continuous wave (CW) light, time-resolved (TR) light, intensity-modulated (IM) light, or any combination thereof.

47. The method of claim 30, wherein the fluorescent light emitted from the patient is collected with a three-dimensional multipoint detection array, displayed on a two-dimensional emitted light array, and imaged with a detector.

48. The method of claim 30, wherein the method is performed dynamically as a function of time.

49. The method of claim 35, wherein the measurement M5 is substituted by a measurement M2 at time 0.

50. The method of claim 30, wherein the image is co-registered with an image obtained by magnetic resonance or computed tomography imaging.

51. The system of claim 1, wherein the multipoint incident illumination array comprises a fiducial, and wherein the fiducial is used to determine the spatial localization of the array on the object.

52. The method of claim 30, wherein the multipoint detection array comprises a fiducial, and wherein the fiducial is used to determine the spatial localization of the array on the object.

53. A method of detecting a cellular abnormality in a patient, the method comprising use of the method of claim 30 with a molecular probe targeted to a particular cellular abnormality.

54. The method of claim 53, wherein the method is used for early detection of disease.

55. The method of claim 54, wherein the disease is cancer, a cardiovascular disease, AIDS, a neurodegenerative disease, an inflammatory disease, or an immunologic disease.

56. A method of assessing the effect of a compound on a specified molecular target, the method comprising the use of the method of claim 30 with a molecular probe that is activated by the molecular target, wherein the probe is contacted to the target, the target is imaged prior to and after contact with the compound, and the corresponding images are compared, wherein a change in the molecular target indicates the compound is effective.

57. The method of claim 56, wherein the specified molecular target is a protease, and the compound is a protease inhibitor.

Molecular NIRF imaging probes for use in new methods

Example 1: Specific enzyme target
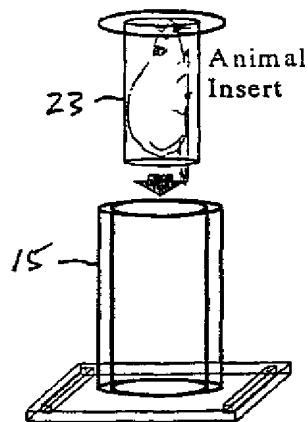

Fig. 1A

Example 2: Specific DNA target

Fig. 1B

Fig. 2A

Fig. 2B

Imaging chamber

Detection fibers

22

Fig. 2C

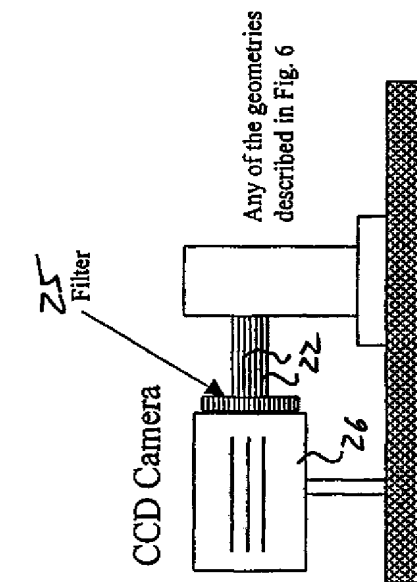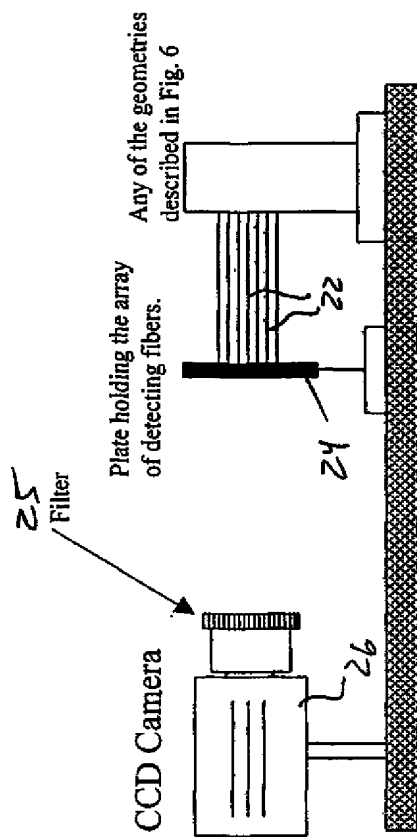Any of the geometries described in Fig. 6

25 Filter

22

26

CCD Camera

Fig. 2E

Any of the geometries described in Fig. 6

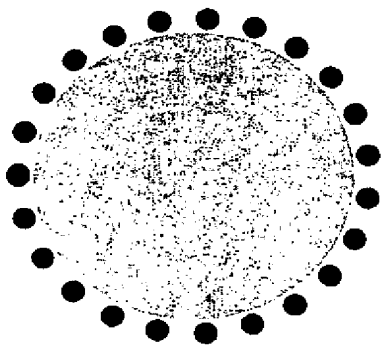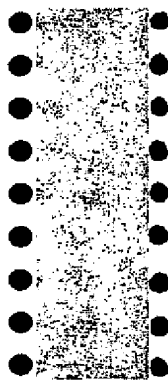Plate holding the array of detecting fibers.
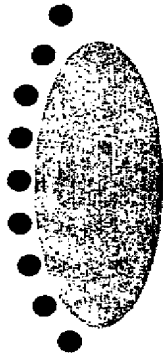
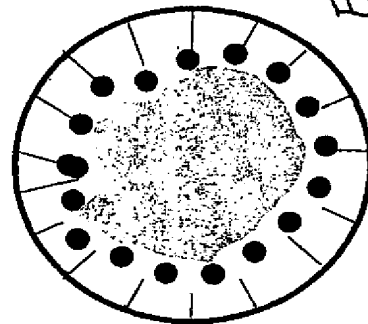25 Filter

22

24

26

CCD Camera

Fig. 2D

Fig. 3C

Fig. 3F

Fig. 3B

Fig. 3E

Fig. 3A

Fig. 3D

Fig. 4B

Fig. 4C

Fig. 4D

Fig. 5

The following text is from the figure (rotated):

M1 — Collect fluorescence measurements — 71

M2 — Collect intrinsic signal measurements — 72

M3 — Collect background "bleed through" signal — 73

M4 — Collect background ambient light signal — 74

M5 — Collect light from the coupling liquid alone (no tissue, no filter) — 75

70

Generate self-calibrated measurement

$$M = \frac{M1-M3}{M2-M4} \quad \text{and} \quad M' = \log\frac{M2-M4}{M5-M4}$$

80a — 80b

Use time-domain data to fit for average optical properties at the emission and excitation wavelength. — 81

Simulate the photon propagation at the emission wavelength for cylindrical geometry — 82

Simulate the photon propagation at the excitation wavelength for cylindrical geometry — 84

Obtain a theoretical (numerical or analytical) forward predictor P of the measurement M, and a forward predictor P' of the measurement M' — 88

Apply DOT principles, namely construct a function $F(U)=(M-P\cdot U)^2$, where U is the vector of unknown concentrations of targeted enzymes at all different positions of the volume under investigation — 90a

Apply DOT principles, namely construct a function $F'(O)=(M'-P'\cdot O)^2$, where O is the vector of unknown concentrations of dye distributed at all different positions of the volume under investigation — 90b

Minimize function F(U) to obtain the distribution and magnitude of U. — 92a

Minimize function F'(O) to obtain the distribution and magnitude of O — 92b

Obtain the activation ratio (AR) image defined as AR=U/O — 93

95

ITERATE

Fig. 4A

Fig. y: Molecular maps

Absorption map

x 10⁻⁸ M

Fig. 6A

Concentration of
molecular probe =
accumulation

Fluorescence map

x 10⁻⁸ M

Fig. 6B

Fluorescence of
molecular probe =
activation

Molecular map
(AR image)

Fig. 6C

Fluorescence activation
image directly correlating
with a given molecular
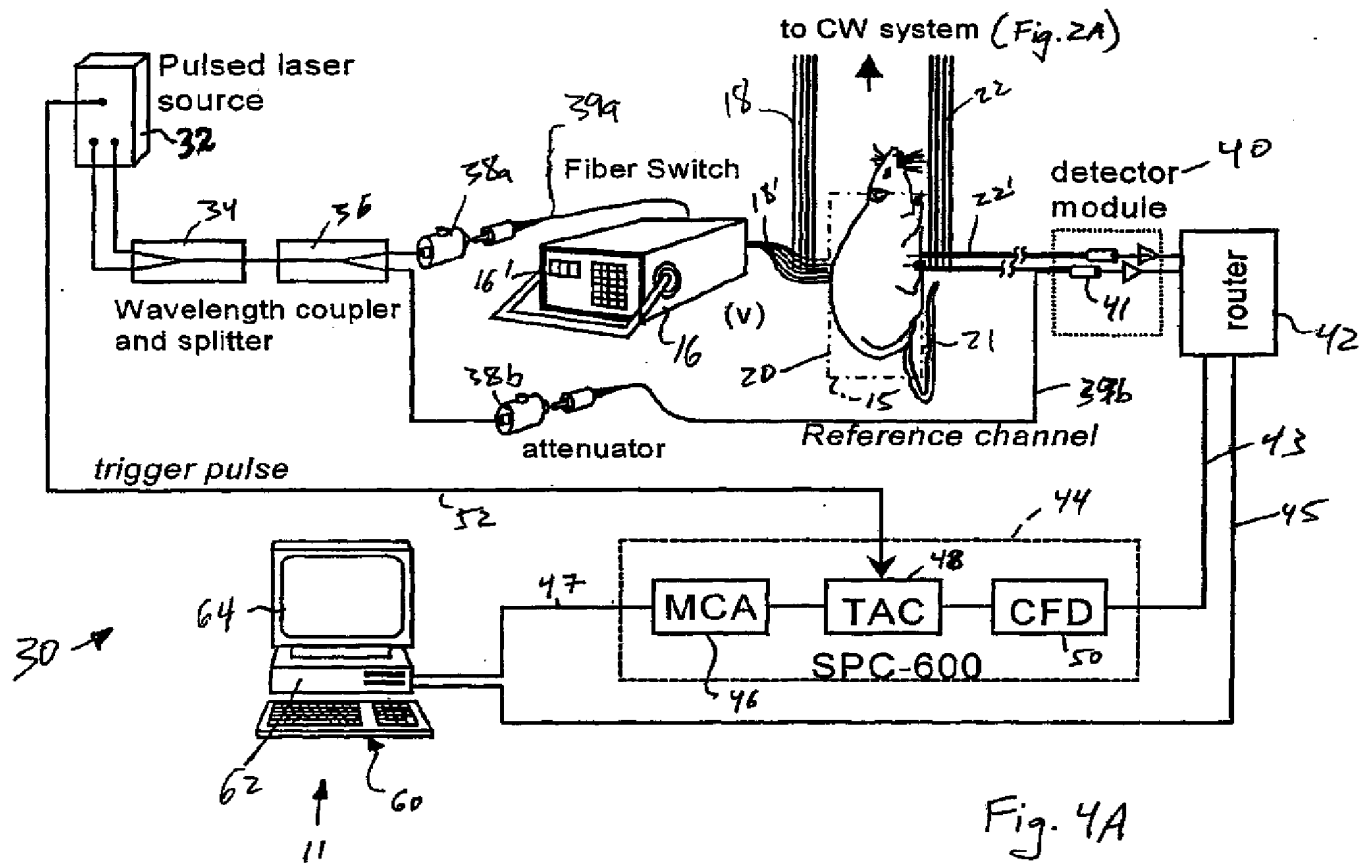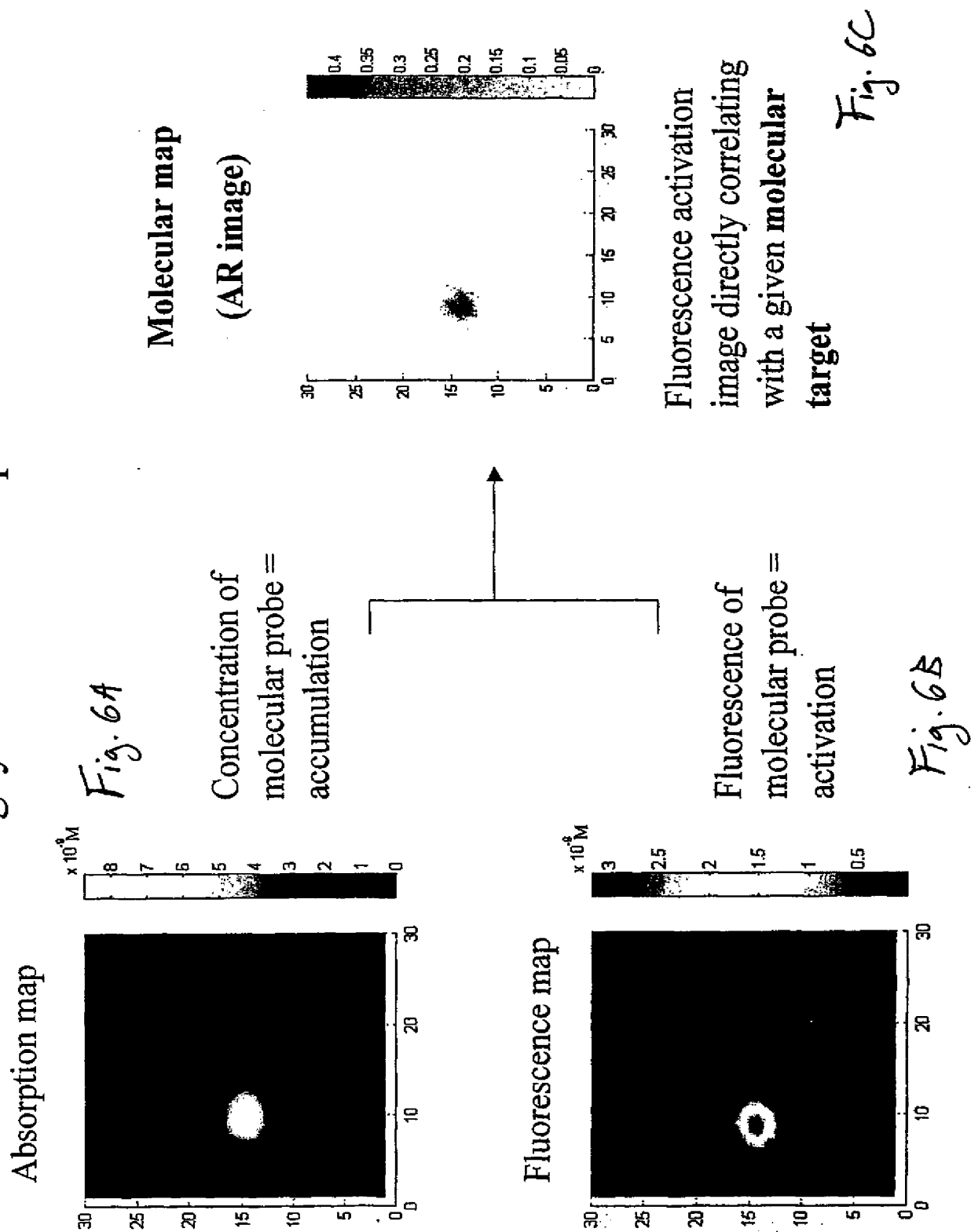target
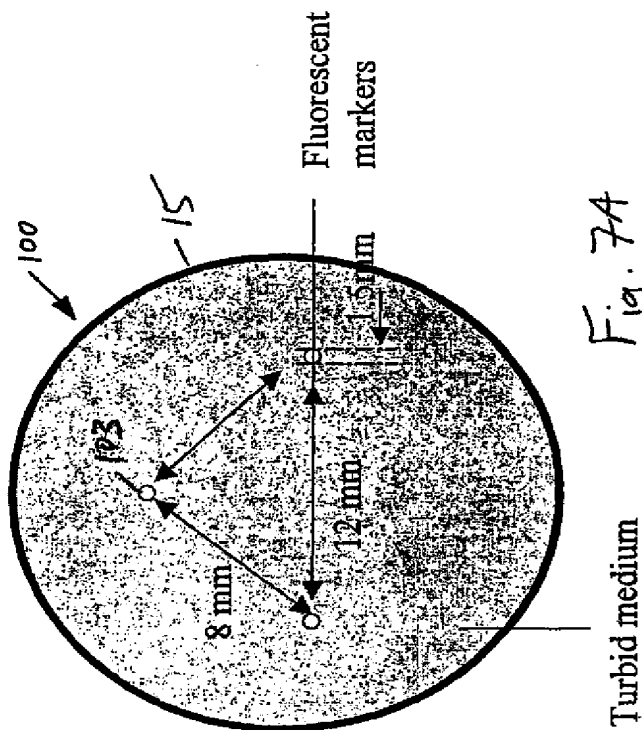
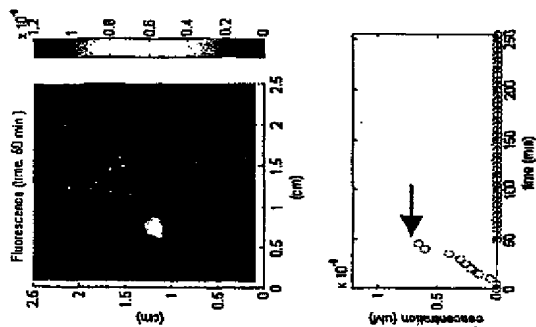B. Reconstructed images

Fig. 7B

A. Phantom set-up

Fig. 7A

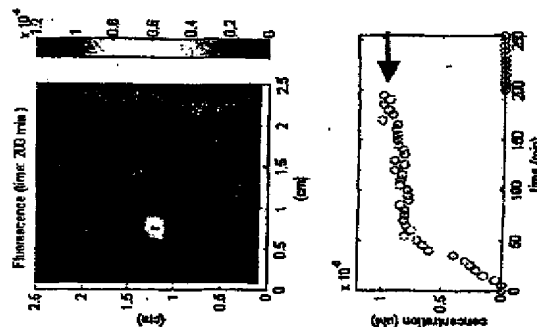Fluorescent markers

Turbid medium

Fig. 8D

Fig. 8C

Fig. 8F

Fig. 8E

Fig. 8A

Fig. 8B

Experimental set-up

3 cm

MRI

FMT images

Fused images

Tumor/level

Fig. 9A

Fig. 9B

Fig. 9C

x10⁻⁸M
2.5
2.0
1.5
1.0
0.5
0.0

Heart level

Fig. 10A

Fig. 10B

x10⁻⁸M
2.5
2.0
1.5
1.0
0.5
0.0

Kidney level

Fig. 11A

Fig. 11B

x10⁻⁸M
2.5
2.0
1.5
1.0
0.5
0.0